Theoretical Notes
Note 192

July 1974

EMP Propagation in the Ionosphere

Kenneth C. Chen
Air Force Weapons Laboratory

and

Joe Martinez
The Dikewood Corporation

Abstract

This note complements an earlier note on the subject in giving analytical formulas for calculating the propagated time waveform of EMP propagation in the ionosphere. Extensive use of the steepest descent integration and geometrical ray theory of propagation makes numerical calculations a minimum. However, as in the previous note, we treat the ionosphere as a linear medium in spite of the powerful pulse involved.

1. Introduction

This note is intended for the simplification of the analysis and numerical computation of a previous note by Messier on "The Ionospherically Propagated Exoatmospheric EMP Environment."[1] In achieving this, analytical formulas and graphical procedures are described through the use of the steepest point integration and geometrical ray theory. However, since it is based on the same physical assumption, the linearity of the medium, they are subject to the same limitations.

In [1] geometrical ray theory is applied to calculate the group delay, the phase shift, and the dispersion; however, it is not applied to the calculation of the time domain waveform, but relies on the complicated numerical inversion of the Fourier transform. Although Brau, et al.[2] gave some analysis to the time domain waveform, the application of stationary phase integration has been limited to where analytical formulas for the location of the saddle point are available. Therefore, the first task of this note is to show how ray theory and saddle point integration can be employed to relieve the pains of numerical computation.[3, 4, 5] Time domain waveforms for an arbitrary stratified ionospheric model are analyzed in detail.

Since this study is concerned with the effect on the satellite system, we neglect the low frequency part of the signal, which is bounced back to the ground to interfere with the ground station. We elaborate on the high altitude ringing modes[6] corresponding to the branch points of the local

index of refraction of the electromagnetic wave, since this can be the dominant phenomenon among all the coupling of energy from EMP to the satellite system.

We assume that the readers are familiar with elementary theory of electromagnetic waves in plasmas. Or, they can consult Messier's note[1] and some textbooks on the subject. We also adopt most notations used in [1].

In Section 2 the problem signal dispersion is described by an inverse Fourier integral. This integral is evaluated by the steepest descent integration. The graphical technique used in conjunction with the steepest descent integration is described. In Section 3 special attention is paid to the tail of the dispersed signal. Of particular importance is the phenomenon that the dispersed signal does depart at a certain time, named as the maximum delay time. This arises from the stratified nature of the index of refraction in the ionosphere. In Section 4 we give the phase, and the envelope of the dispersed signal at four different attitudes for nighttime and daytime ionosphere. This complements earlier studies of Messier. These envelopes are not valid near the wavefront. The wavefront is described by Sommerfeld's precursor, which we describe in Section 5.

Other notes on the subjects are on the consideration of spherical ionosphere [7, 8, 9, 10] and solutions based on expansions around the carrier frequency. [11]

2. Analytical Formulas for Time Domain Waveform of a Propagating Pulse in the Ionosphere

Consider an EMP, $g(t)$, entering into the ionosphere. Let the spectrum of such an incident pulse be $\tilde{g}(\omega)$, then

$$\tilde{g}(\omega) = \int_o^\infty g(t)\, e^{-i\omega t}\, dt \tag{2.1}$$

Let the ionosphere transmission function be given by

$$T(\omega) = e^{-i\frac{\omega}{c}\int_o^x n(x', \omega)dx'} \tag{2.2}$$

Here $n(x', \omega)$ is the local index of refraction at x'. For isotropic cold plasmas n is given by

$$n(x, \omega) = \left[1 - \omega_p^2(x)/\omega^2\right]^{1/2} \tag{2.3}$$

$\omega_p^2 = \frac{Nq^2}{m_e \epsilon_o} = 3182.8N$ = plasma frequency

$q = 1.602 \times 10^{-19}$ coul = electronic charge

$\epsilon_o = 8.842 \times 10^{-12}$ farad/m = permittivity of free space

$m_e = 9.108 \times 10^{-31}$ Kg = electronic mass

N = local electron density

The dispersed time domain waveform at x is given by[1]

$$E(t) = \frac{1}{2\pi}\int_{-\infty}^{\infty} \tilde{g}(\omega)T(\omega)\, e^{i\omega t}\, d\omega$$

$$= \frac{1}{2\pi}\int_{-\infty}^{\infty} \tilde{g}(\omega)\, e^{i\omega\left[t-\frac{1}{c}\int_0^x n(x',\,\omega)dx'\right]}\, d\omega \qquad (2.4)$$

Messier discussed phase delay, group delay and the dispersion based on ray theory. Here we steepest descent integrate (2.4) to justify the use of ray theory and also to give analytical formulas for the dispersed time domain waveform. Referring to an elementary discussion of saddle point integration given in [12], we have the saddle points of (2.4) as the solutions to

$$\frac{d}{d\omega}\left[\omega\int_0^x n(x',\,\omega)dx'\right] = ct$$

or

$$\int_0^x \frac{dx'}{n} = ct \qquad (2.5)$$

On assuming no two saddle points are close to each other, we have the formula for the contribution from each saddle point as

$$\frac{1}{2\pi}\tilde{g}(\omega_s)\left\{\frac{2\pi i}{\frac{d^2}{d\omega^2}\left[\omega\int_o^x n(x',\omega)dx'\right]\Big|_{\omega=\omega_s}}\right\}^{1/2} e^{i\omega_s t - i\int_o^x \omega_s(x',\omega_s)dx'} \tag{2.6}$$

Let us introduce dispersion, D, as follows:

$$D = \frac{d^2}{d\omega_s^2}\,\omega_s\int_o^x n(x',\omega_s)dx'$$

$$= \int_o^x \left(\frac{1}{n^2} - 2\right)\frac{\omega_p^2}{n\omega_s^3}\,dx' \tag{2.7}$$

Further, we denote

$$\phi = \omega_s t - \int_o^x \omega_s n(x',\omega_s)dx' \tag{2.8}$$

In the analysis of Brau, et al.[2] of time domain waveforms by method of stationary phase an expansion is carried out for the index of refraction with the assumption that $\omega_p << \omega$. Such an expansion limits the validity of the analytical formulas to only sufficiently earlier time. Note also that Sommerfeld precursor describes the wavefront.[3, 13] Therefore, the envelope so obtained is applicable to some small time interval (Fig. 2.1). To remedy such a deficiency we use a graphical method,[3, 4, 5] which avoids the use of expansion of the refractive index.

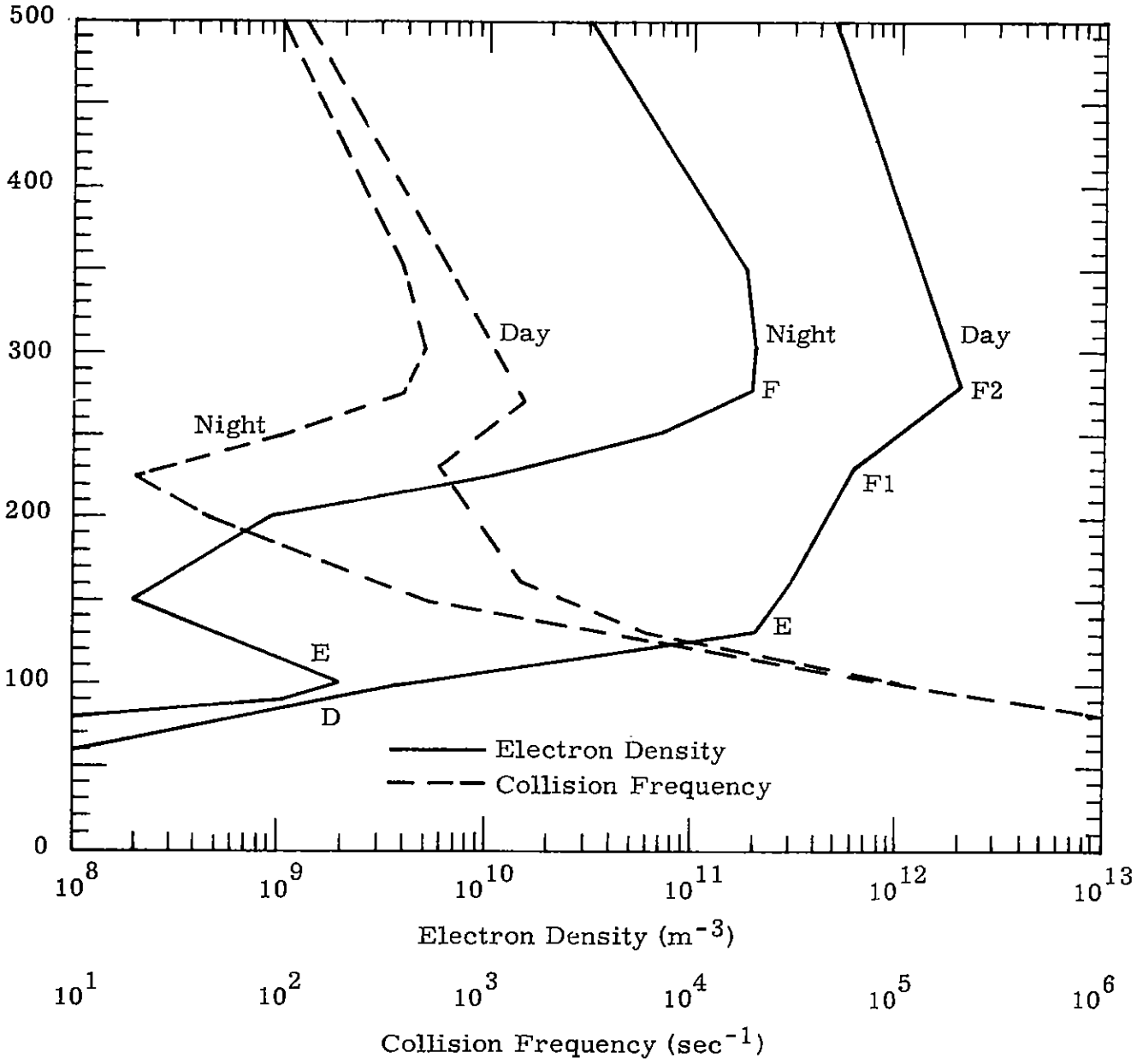

Figure 2.1. Ionospheric Models

Instead of solving (2.5) to yield the value of saddle point at time t, we study inversely the values of t, D and ϕ corresponding to each chosen ω_s. Once representative values of ω_s are obtained, the envelope of the time domain waveform of a dispersed pulse can be graphed.

3. Analysis of Contribution due to Saddle Points Near Cutoff Frequency: Study of Tails of Dispersed Pulses

Analysis of (2.5) shows that the saddle points near the cutoff frequency contribute to the tails of the dispersive pulses. In order to gain more insight into these tails, it is helpful to study some simple profile of electron density. Since the time delay due to the saddle points near the cutoff comes mostly near the observation point, we can approximate in such a small interval by some profiles. An examination of the electron density profile of the ionosphere (Fig. 2.1) reveals that at an altitude of 100 Km at nighttime and at an altitude of 200 KM in the daytime the profiles are linear. Therefore, it is worthwhile to look into a linear profile for these two situations.

Let us study (2.5) which gives the time corresponding to the arrival of the contribution from a saddle point ω_s

$$ct = \int_o^x \frac{dx}{n}, \qquad n = \left(1 - \frac{\omega_p^2}{\omega_s^2}\right)^{1/2} \tag{3.1}$$

Thus, the time delay compared to a pulse propagating in free space is

$$c\Delta t = \int_o^x \left(\frac{1}{n} - 1\right) dx \tag{3.2}$$

with $c\Delta t$ measured in m.

Using a linear profile (Fig. 3.1), we locally approximate ω_p^2 as follows:

$$\omega_p^2 = \frac{Nq^2}{m\epsilon}[1 - A(x_o - x)] \tag{3.3}$$

Let ω_c be the cutoff angular frequency for n at x_o, then

$$\frac{\omega_p^2}{\omega_c^2} = 1 - A(x_o - x) \tag{3.4}$$

which leads to $n(x_o, \omega_c) = 0$ as required by the definition of a cutoff angular frequency.

The time delay for the contribution due to the saddle point ω_s from x to x_o is

$$\Delta t = \int_x^{x_o} \frac{dx'}{\left[1 - \frac{\omega_c^2}{\omega^2} + \frac{\omega_c^2}{\omega^2} A(x_o - x')\right]^{1/2}} - (x_o - x)$$

$$= 2\frac{\left[1 - \frac{\omega_c^2}{\omega^2} + \frac{\omega_c^2}{\omega^2} A(x_o - x)\right]^{1/2} - \left[1 - \frac{\omega_c^2}{\omega^2}\right]^{1/2}}{\frac{\omega_c^2}{\omega^2} A} - (x_o - x) \tag{3.5}$$

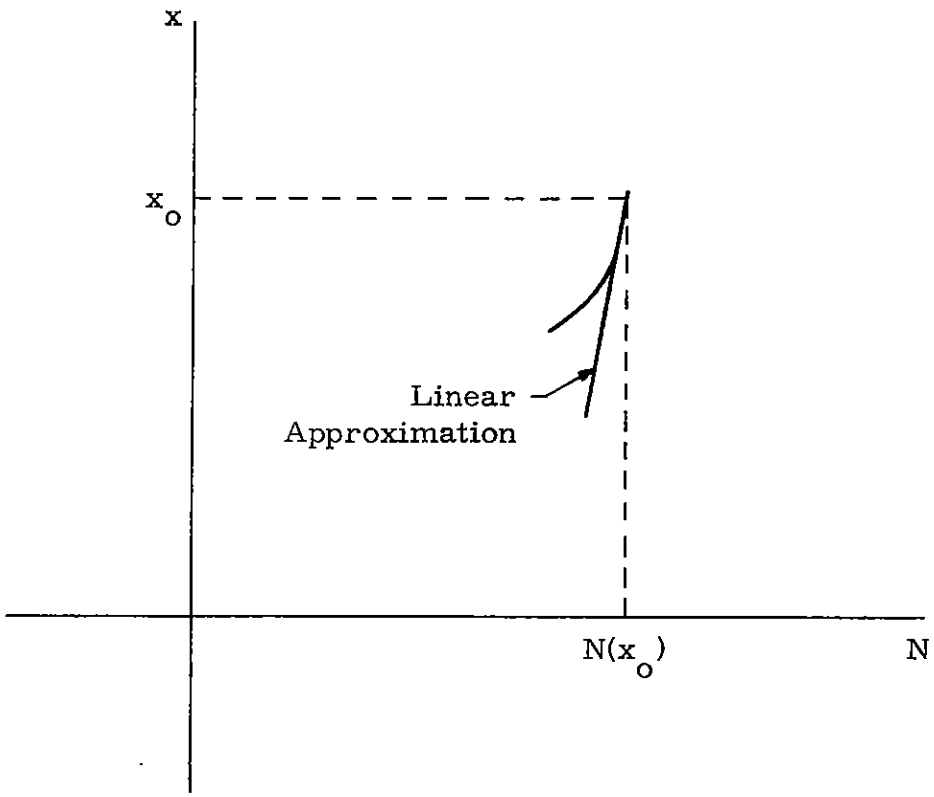

Figure 3.1. The Approximation for n Near Cutoff

Here

$$A = \frac{1}{N}\frac{dN}{dx}\bigg|_{x=x_o} = \frac{N(x_o) - N(x)}{N(x_o)(x_o - x)} \tag{3.6}$$

which follows from (3.4). Let us give two numerical examples.

1. Nighttime at an altitude of 100 Km

$$N_o = N(x_o) = 2 \times 10^9$$

$$A = \frac{2 \times 10^9 - 1 \times 10^9}{2 \times 10^9 \times 10} = \frac{1}{20} \times 10^{-3}\ m^{-1}$$

At $\omega_s = \omega_c$, the time delay is maximum. Thus,

$$c\Delta t_{max} = \int_{9x10^4 m}^{10x10^4 m} \left(\frac{1}{n} - 1\right) dx = 18.28 \times 10^3\ m$$

$$= \frac{18.28}{3 \times 10^8}\ \mu sec = 60.9\ \mu sec$$

Let us give a table, which shows the delay time corresponding to the contribution from some typical saddle points.

ω/ω_c	2.236	1.414	1.195	1.118	1.054	1.
$(\omega_c/\omega)^2$	0.2	0.5	0.7	0.8	0.9	1.
$c\Delta t$ in 10^3 m	0.84	2.712	4.771	6.365	8.906	18.28
Δt in μsec	2.8	9	15.9	21.216	29.68	60.9

Table 3.1

The maximum delay time, which is the delay time corresponding to the cutoff frequency, is an important quantity for studying pulse propagation in dispersive media with stratification. It is the departure time; for time greater than this maximum delay time the disturbance disappears. This phenomenon does not occur in the case of homogeneous dispersive media, since the system allows infinite delay time at any observation point. [5]

2. Daytime at an altitude of 200 Km

$$N_o = N(x_o) = 4.7 \times 10^{11}$$

$$A = \frac{3 \times 10^{11}}{4.7 \times 10^{11} \times 70} = \frac{3}{329}$$

$$\Delta t_{max} = 300 \times 10^3 \text{ m} = 10^3 \ \mu\text{sec}$$

Let us also show typical delay time in Table 3.2.

ω/ω_c	2.236	1.414	1.195	1.118	1.054	1
$(\omega_c/\omega)^2$	0.2	0.5	0.7	0.8	0.9	1
Δt in 10^3 m	49.44	59.7	71.	79.7	93.6	300
Δt in μsec	164.8	199.	236.6	265.8	312.1	1000

Table 3.2

4. Exoatmospheric Time Waveforms

In this section, we study the dispersed pulse at four different altitudes for two input pulses. They are:

Pulse 1 as shown in Fig. 4.1.

$$g(t) = E_o[e^{-\beta t} - e^{-\alpha t}] \tag{4.1}$$

with

$$E_o = 1$$

$$\alpha = 4.76 \times 10^8 \text{ sec}^{-1}$$

$$\beta = 4 \times 10^6 \text{ sec}^{-1}$$

The unit given here and henceforth in all figures is in volt/m.

The transform of pulse 1 is

$$\tilde{g}(\omega) = E_o\left[\frac{1}{\beta + i\omega} - \frac{1}{\alpha + i\omega}\right] \tag{4.2}$$

Pulse 2 as shown in Fig. 4.1 is

$$g(t) = E_o \frac{d\, e^{\alpha t}}{1 + e^{\beta (t-t_p)}} \tag{4.3}$$

with

$$E_o = 1$$

$$d = 4.6 \times 10^{-7} \quad ,$$

$$\alpha = 4.402 \times 10^8$$

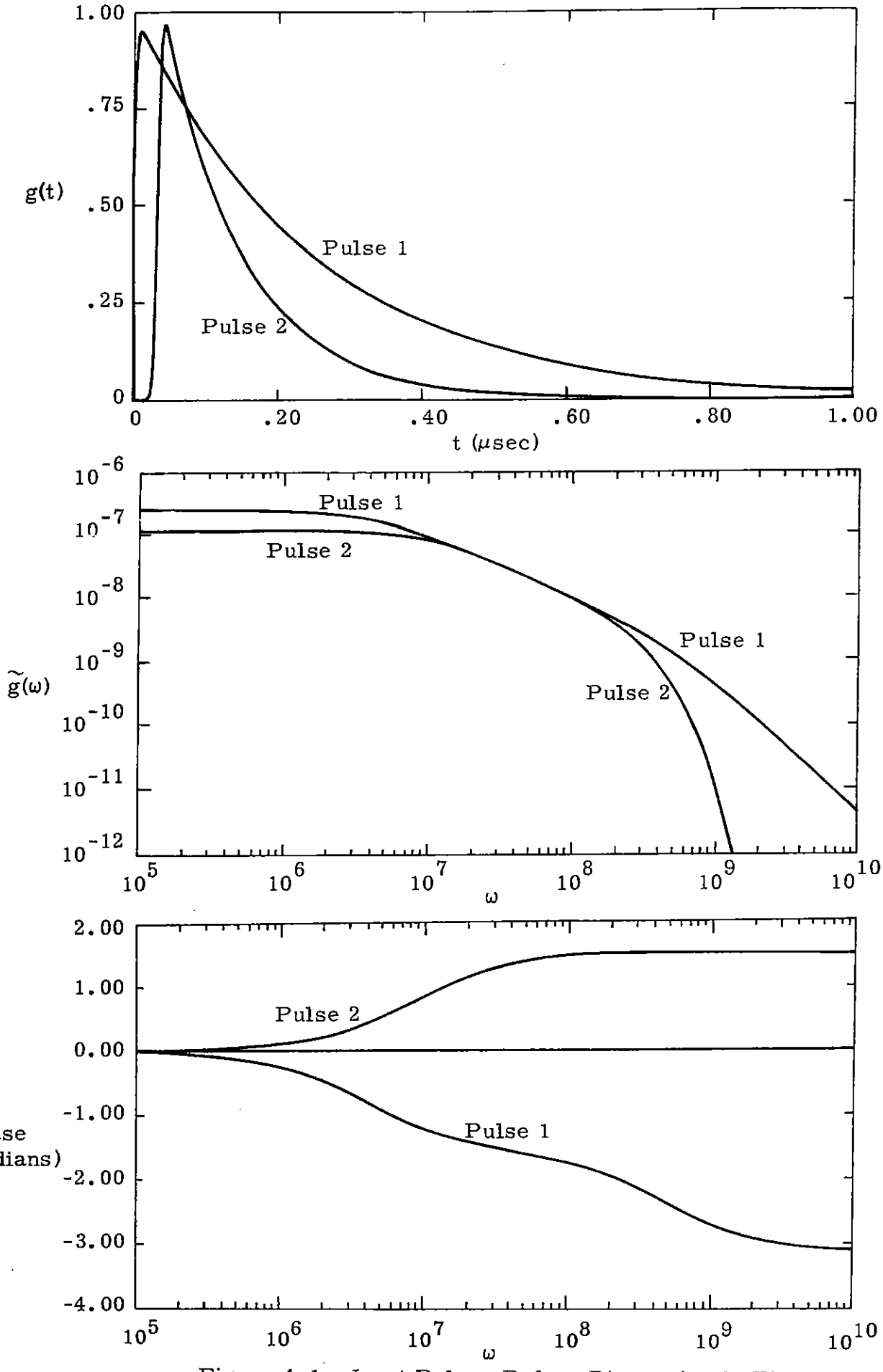

Figure 4.1. Input Pulses Before Dispersion in Time and Frequency Domains

$$\beta = 4.4918 \times 10^{8}$$

$$t_p = 3.33 \times 10^{-8}$$

The transform for pulse 2 given in the Appendix is

$$\tilde{g}(\omega) = E_o \frac{\pi d}{\beta} \frac{e^{\alpha t_p} e^{i\omega t_p}}{\sin(\alpha + i\omega)\frac{\pi}{\beta}} \tag{4.4}$$

$$= E_o \frac{\pi d}{\beta} \frac{e^{\alpha t_p} e^{i\phi_g + i\omega t_p}}{\left[\sin^2 \frac{\pi\alpha}{\beta} \cosh^2 \frac{\pi\omega}{\beta} + \cos^2 \frac{\pi\alpha}{\beta} \sinh^2 \frac{\pi\omega}{\beta}\right]^{1/2}} \tag{4.5}$$

where

$$\phi_g = \tan^{-1}\left(\frac{-\tanh\left(\frac{\omega\pi}{\beta}\right)}{\tan\left(\frac{\alpha\pi}{\beta}\right)}\right) \tag{4.6}$$

We also show ϕ_g and the phase of pulse 1 in Fig. 4.1.

Note that the spectra (4.2) and (4.4) introduce poles when applying the steepest descent integration. However, the residuals due to these poles are exponentially small and there is no need to calculate them. Also, there are two saddle points located symmetrically with respect to the imaginary axis. The late envelope obtained from (2.6) is

$$E = \frac{1}{\pi} \left|\tilde{g}(\omega)\right| \left(\frac{2\pi}{|D|}\right)^{1/2} \tag{4.7}$$

Here D is given by (2.7). The phase delay for the propagating medium is given by (2.8).

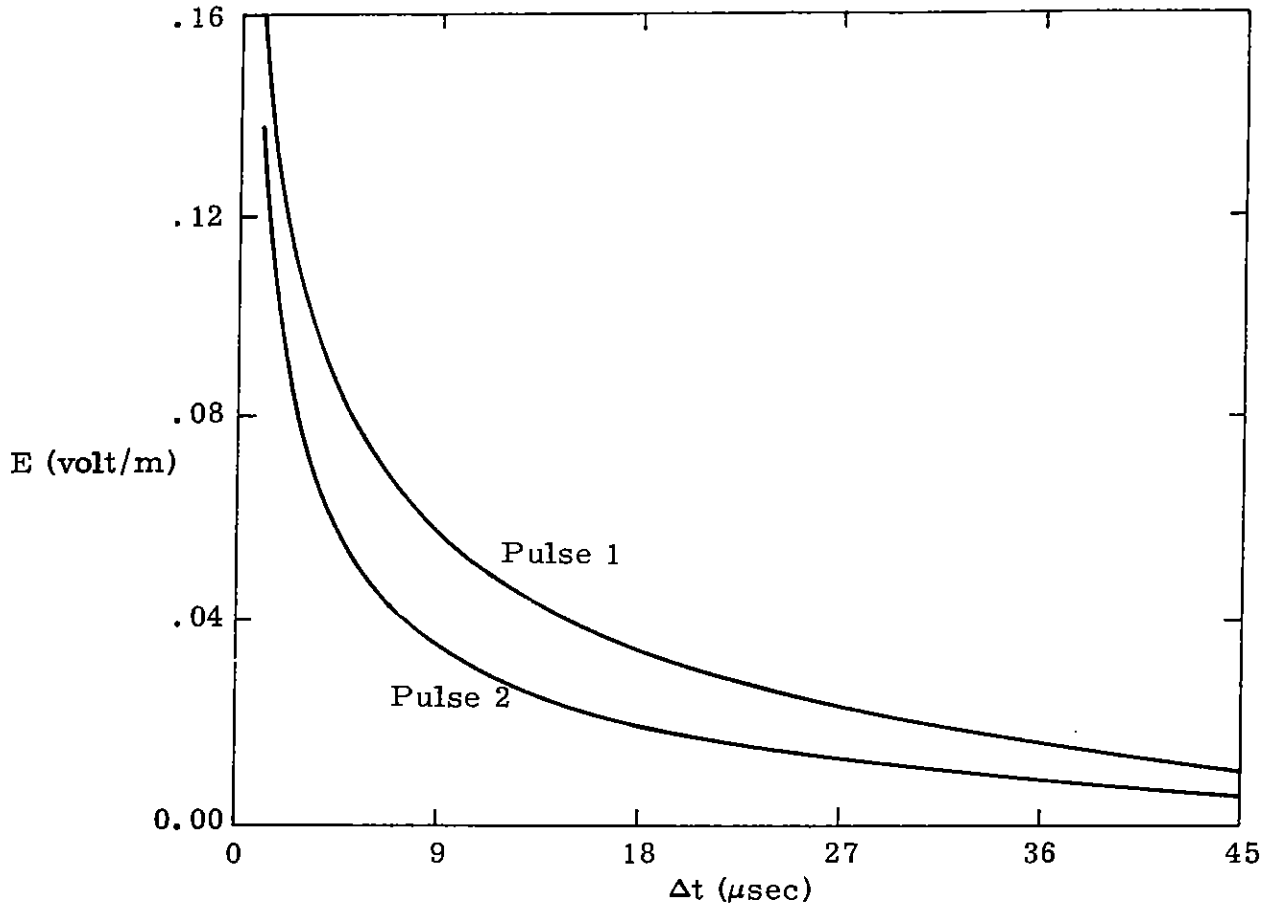

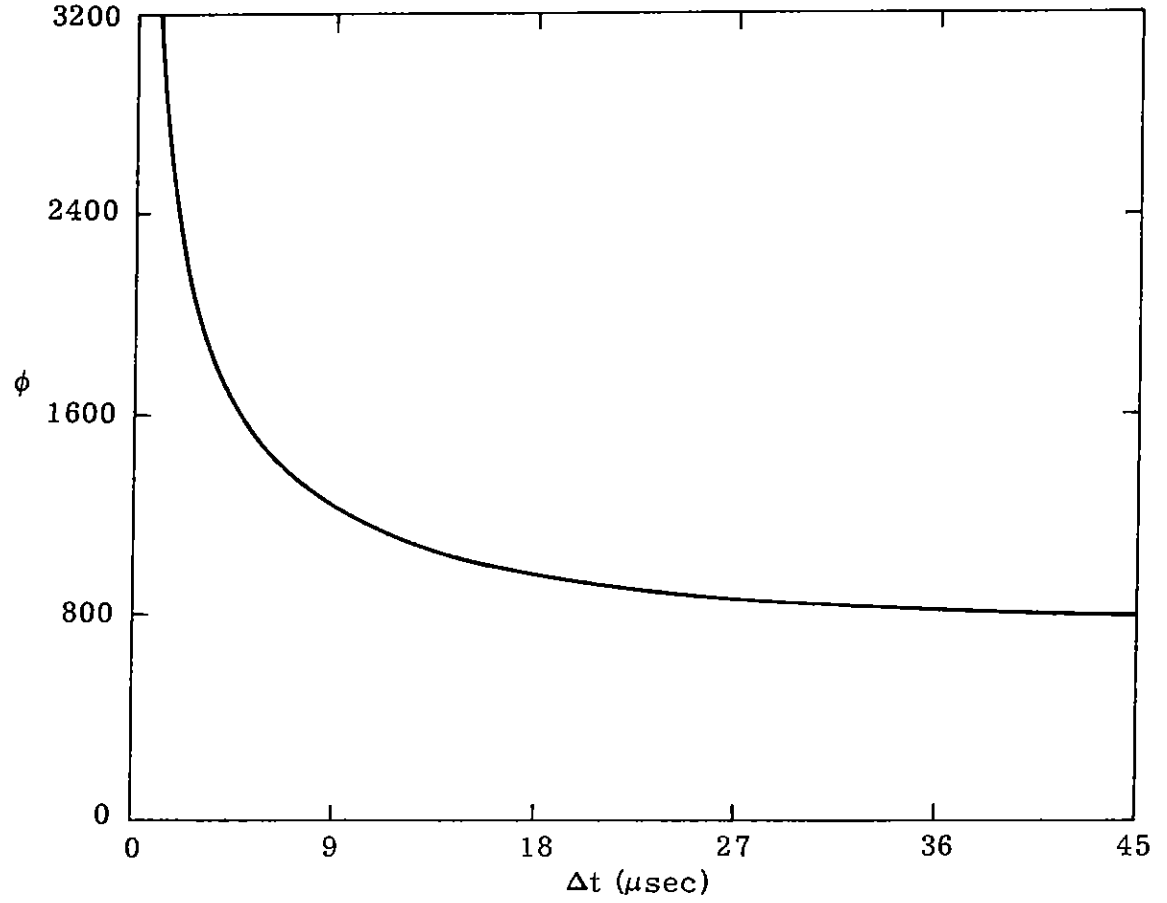

Figure 4.2. Dispersed Pulse with Nightime Ionosphere at 100 km

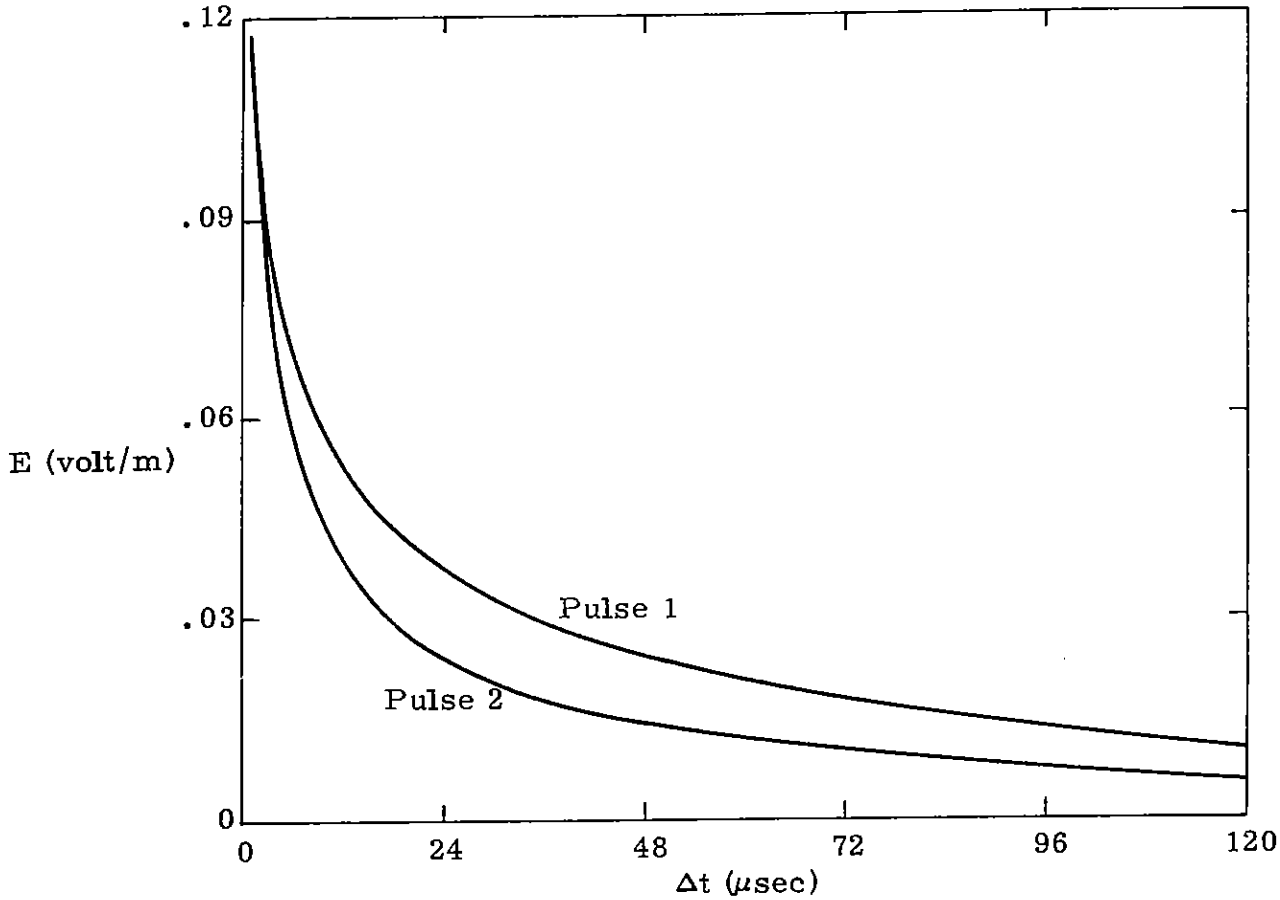

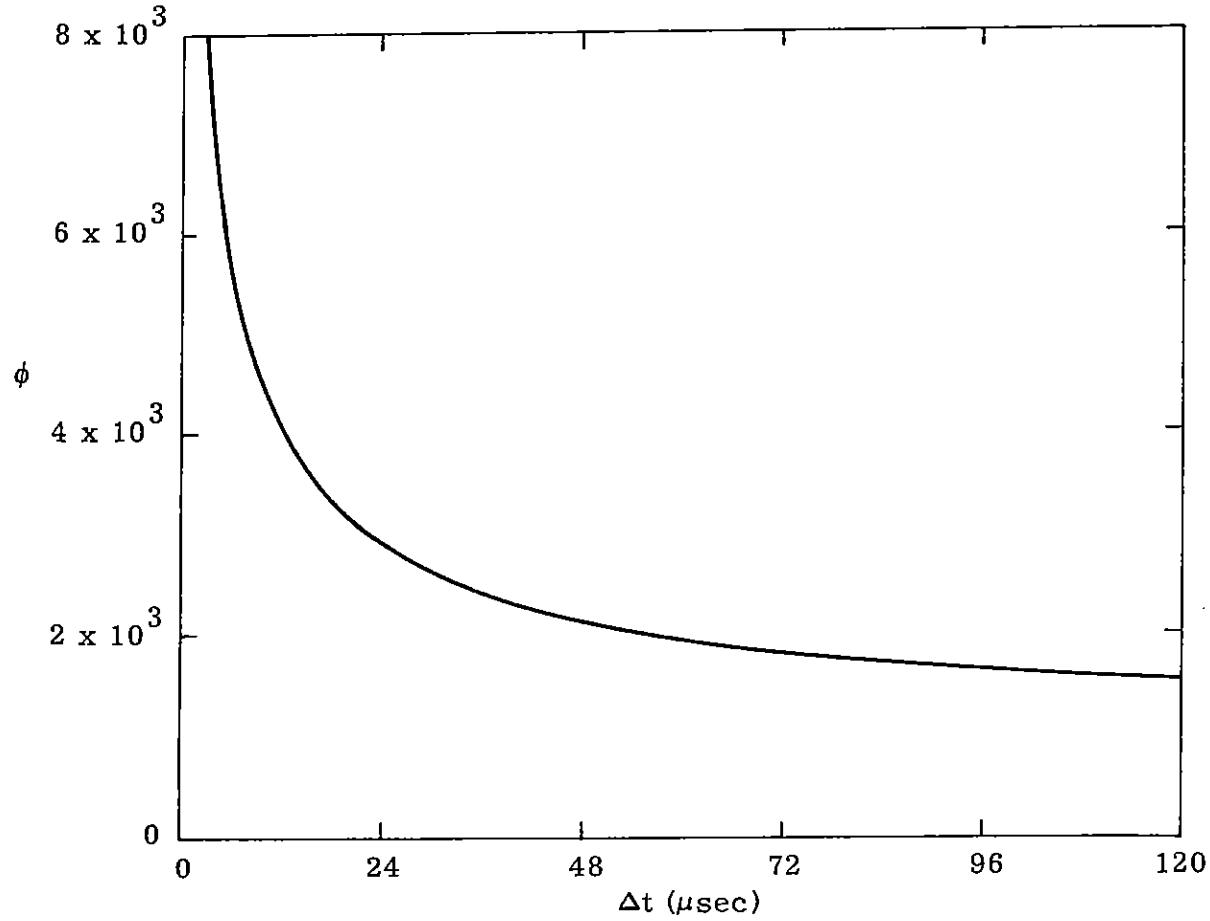

Figure 4.3. Dispersed Pulse with Nightime Ionosphere at 200 km

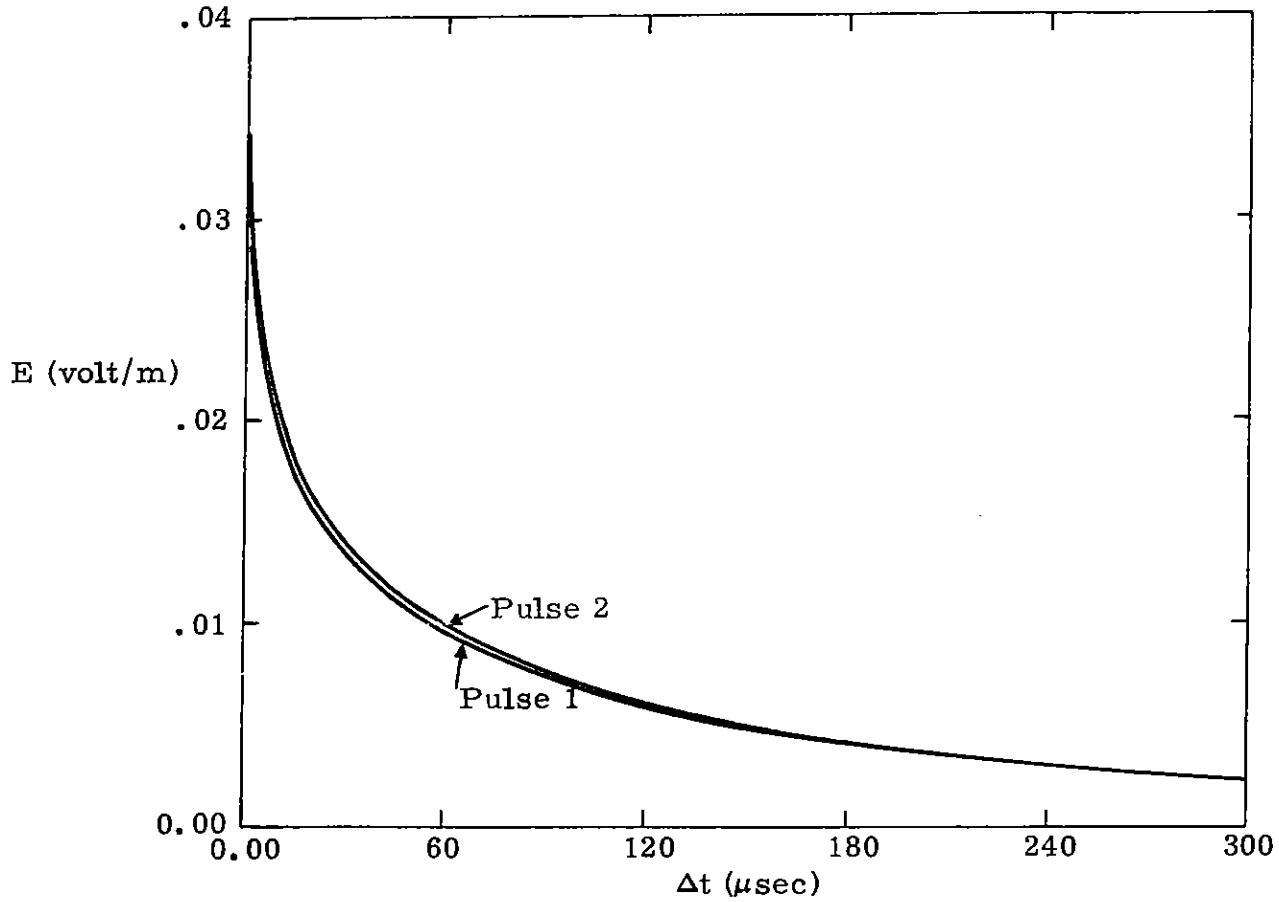

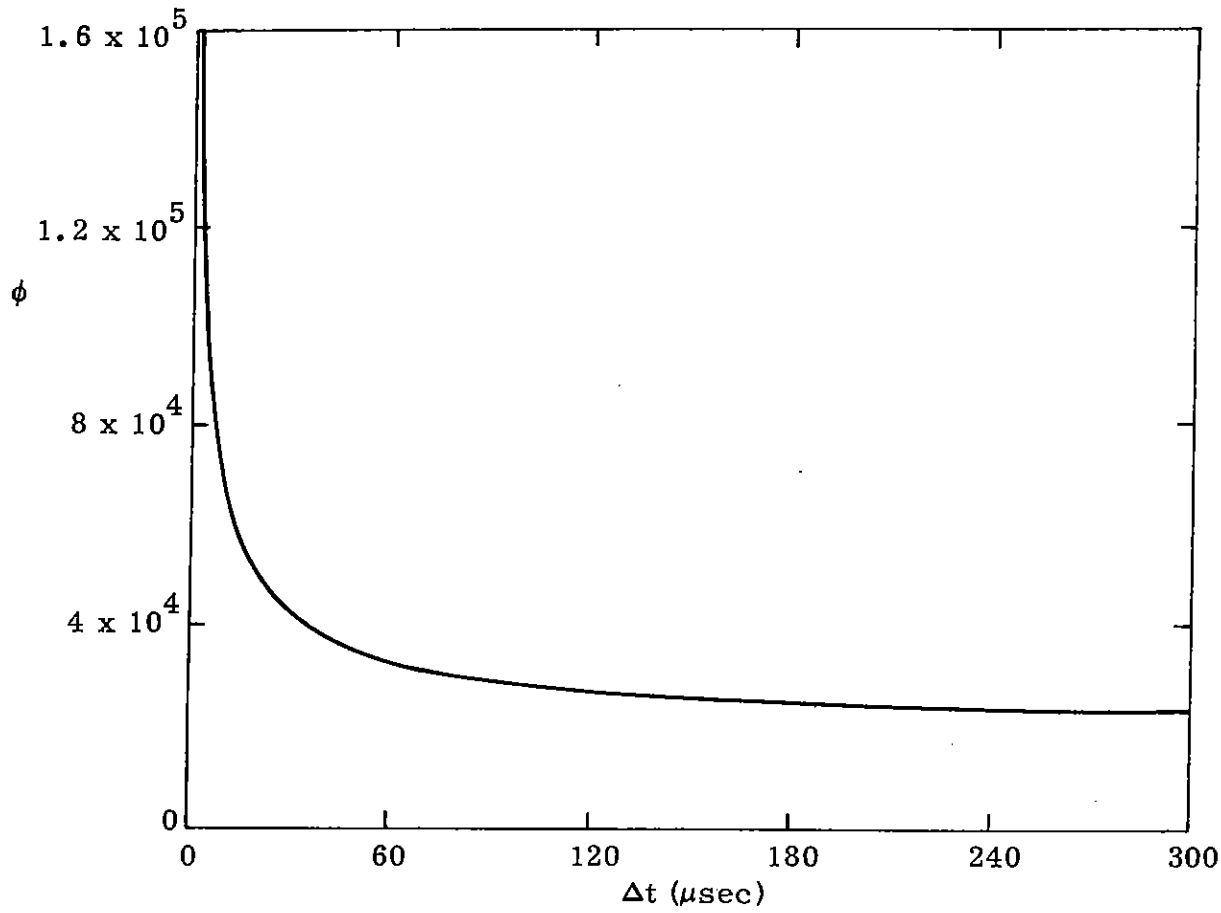

Figure 4.4. Dispersed Pulse with Nightime Ionosphere at 300 km

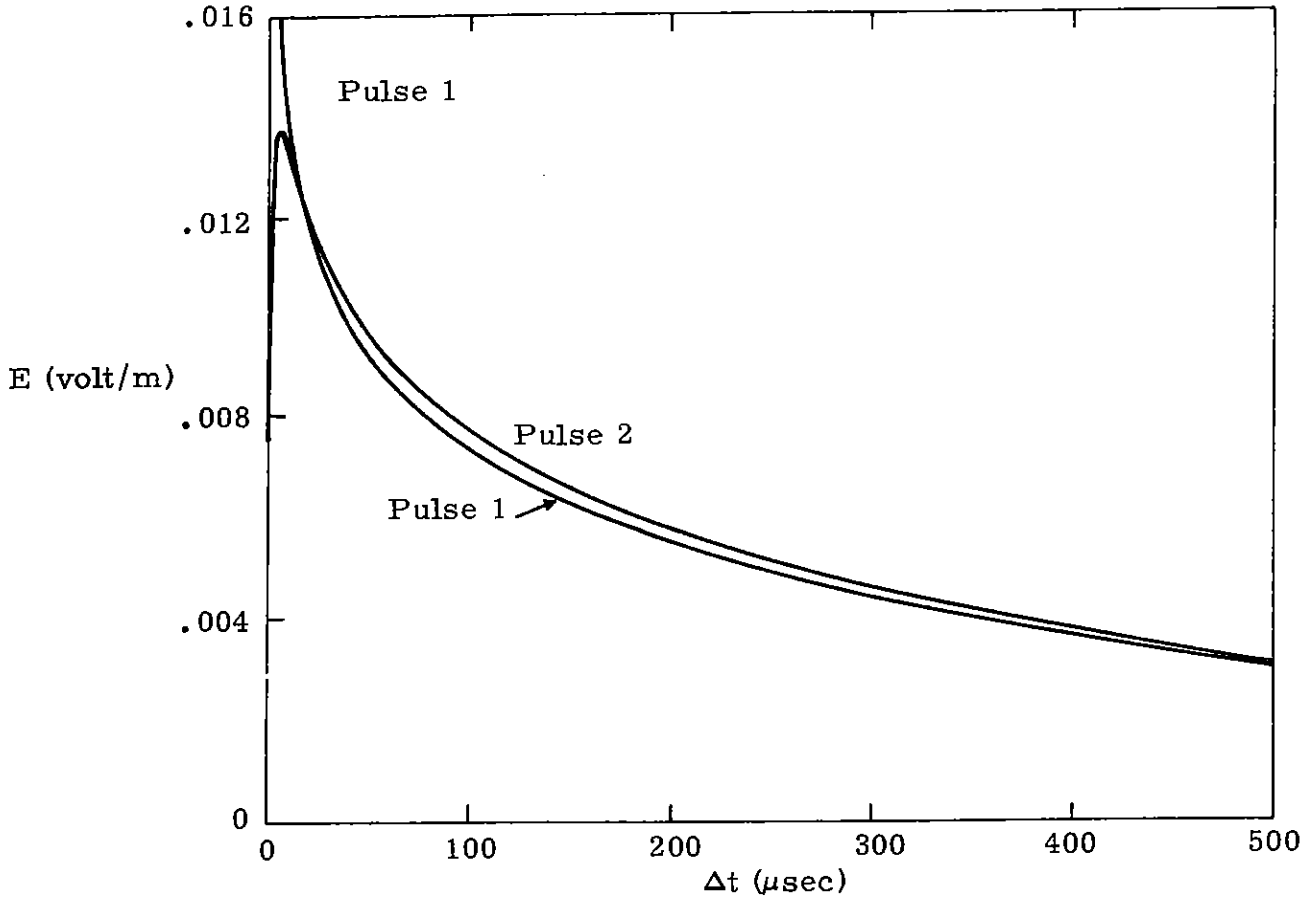

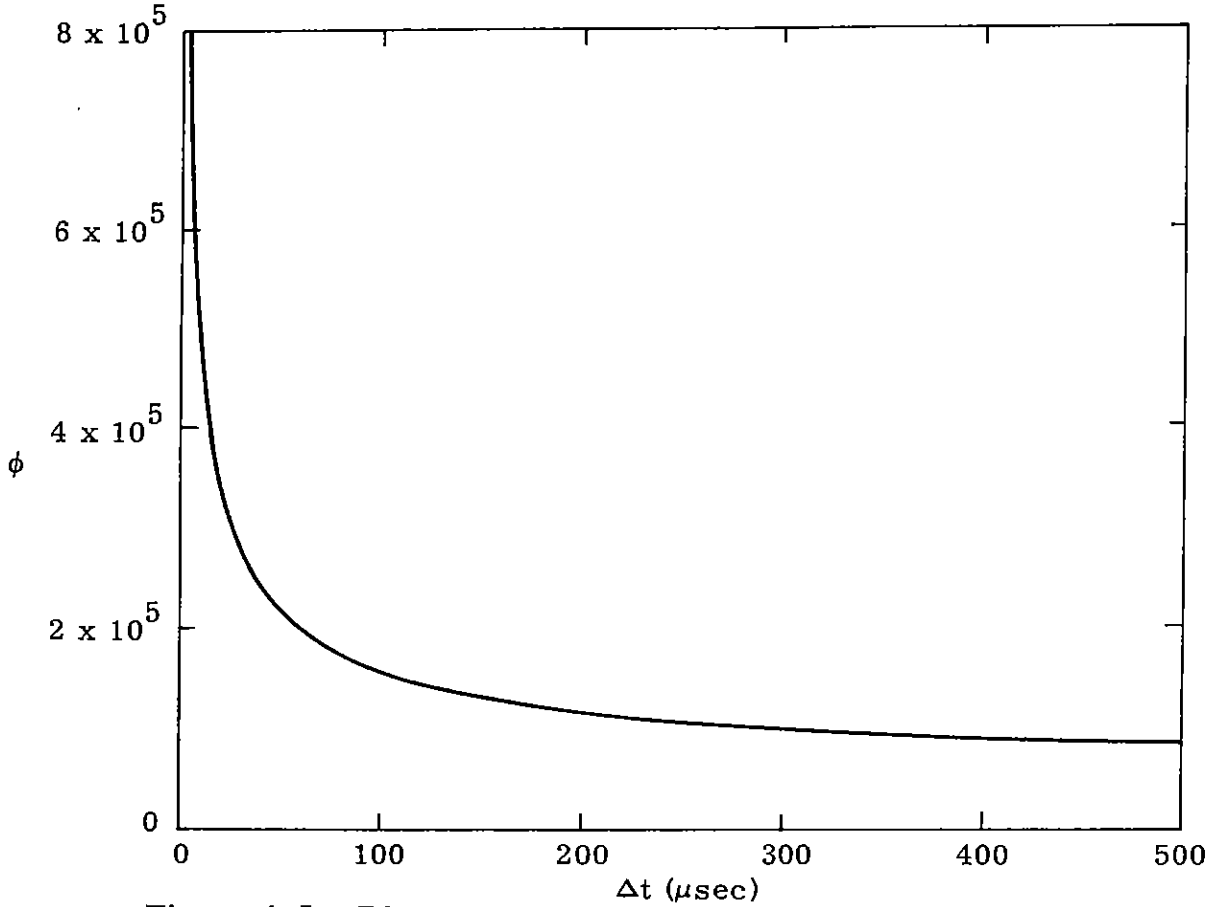

Figure 4.5. Dispersed Pulse with Nightime Ionosphere at 1000 km

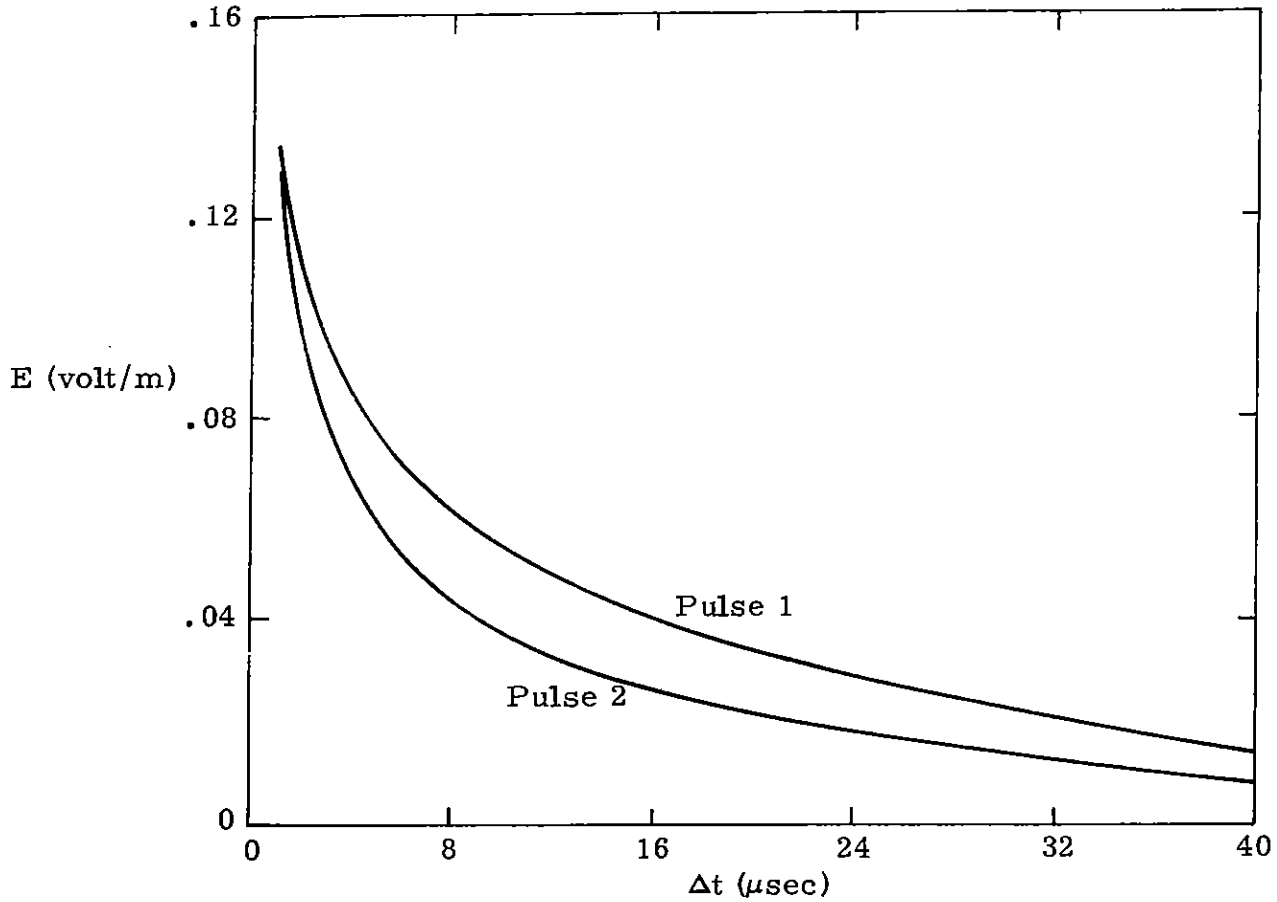

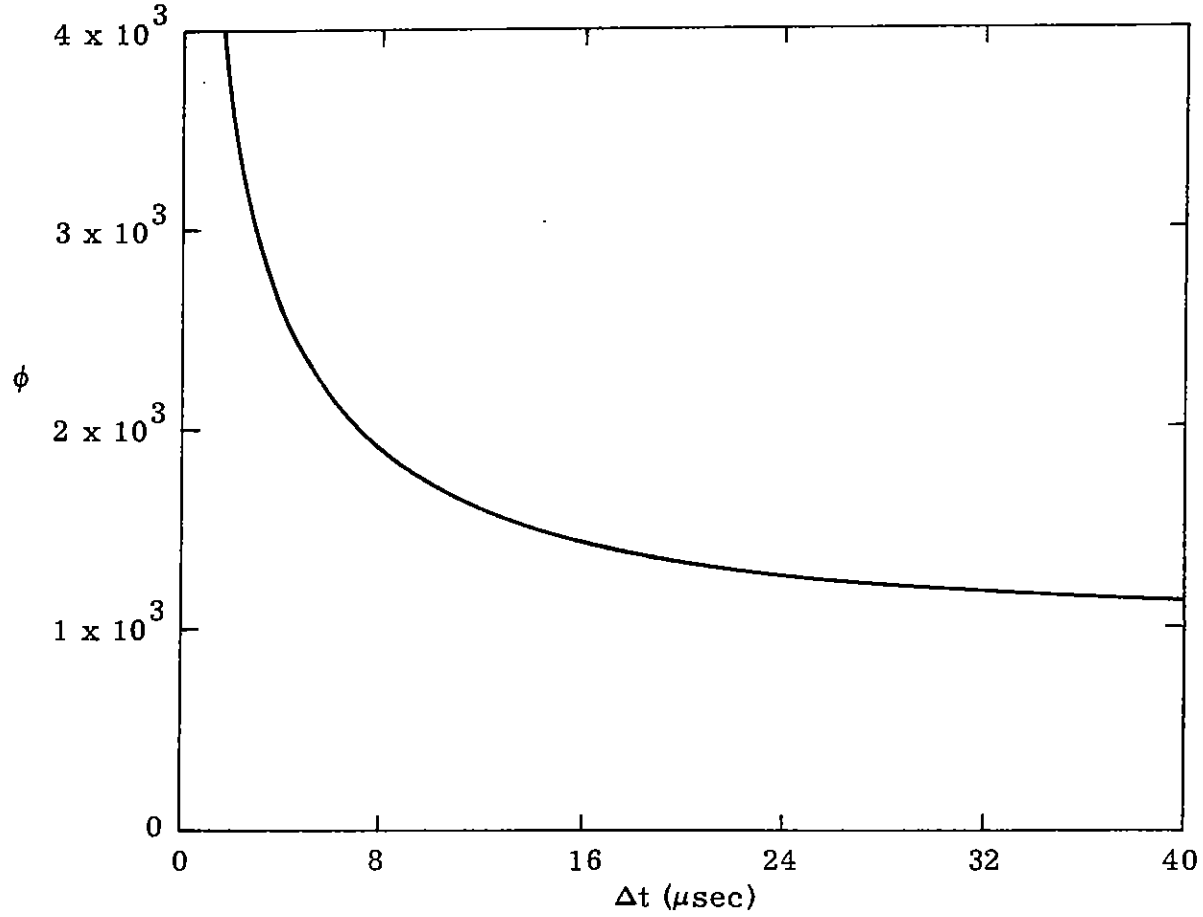

Figure 4.6. Dispersed Pulse with Daytime Ionosphere at 100 km

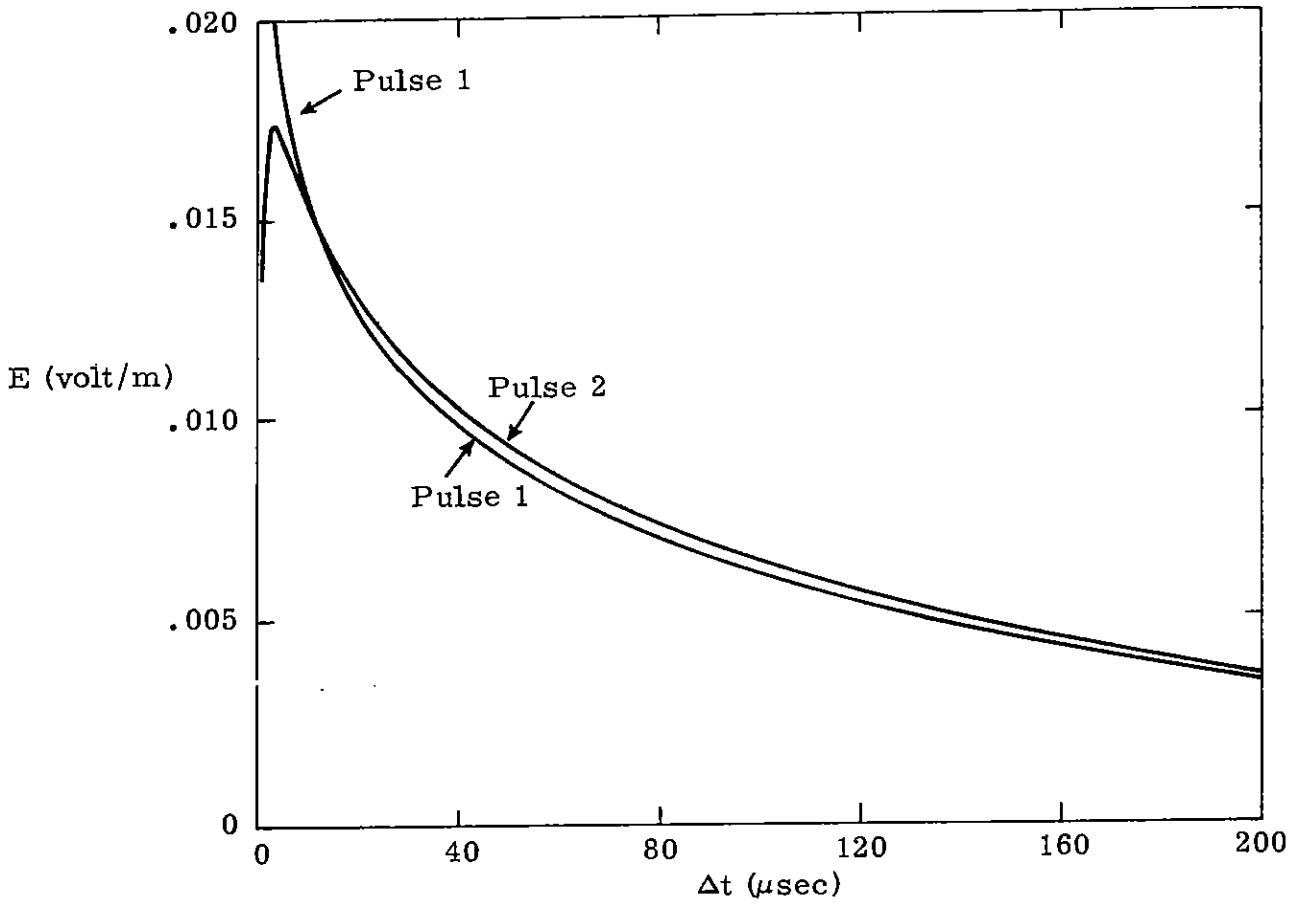

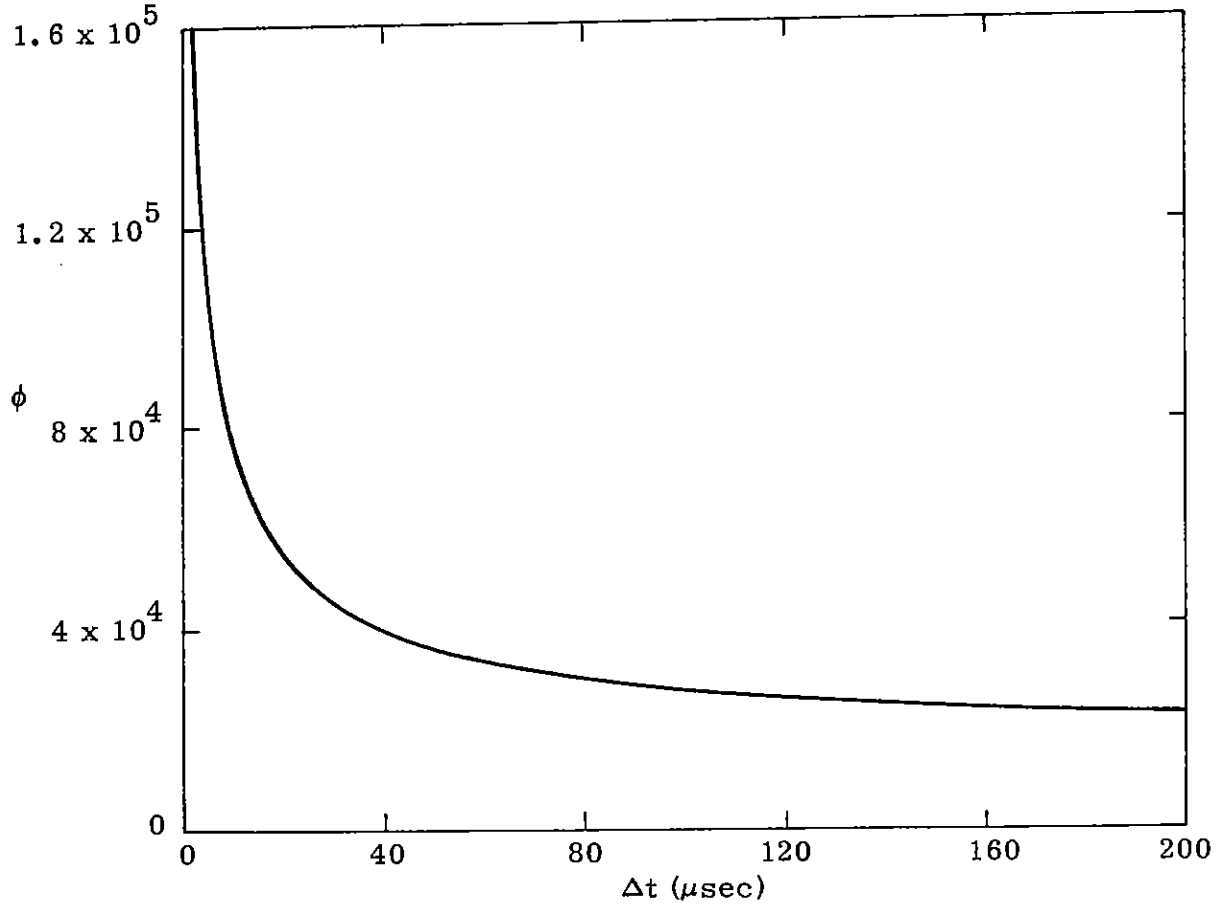

Figure 4.7. Dispersed Pulse with Daytime Ionosphere at 200 km

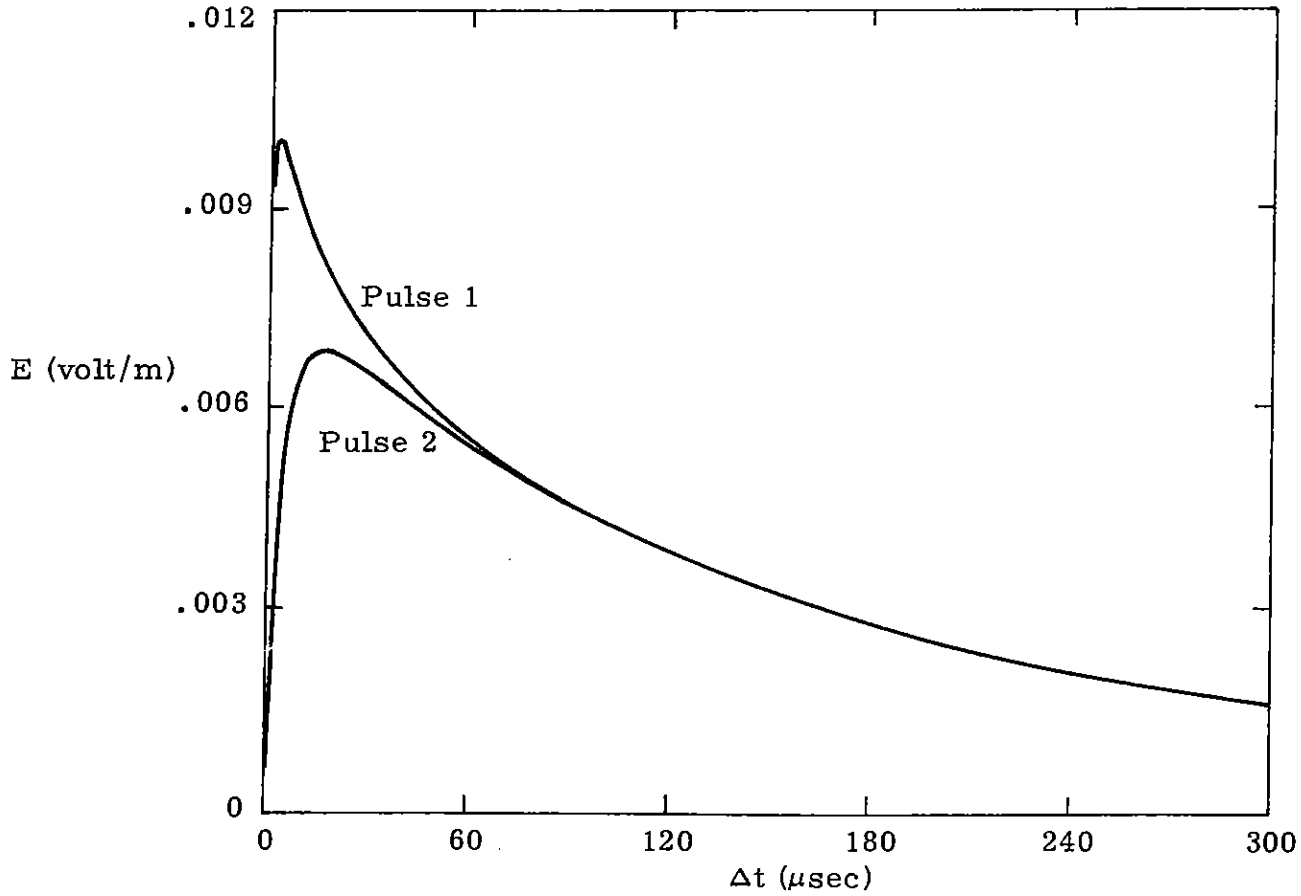

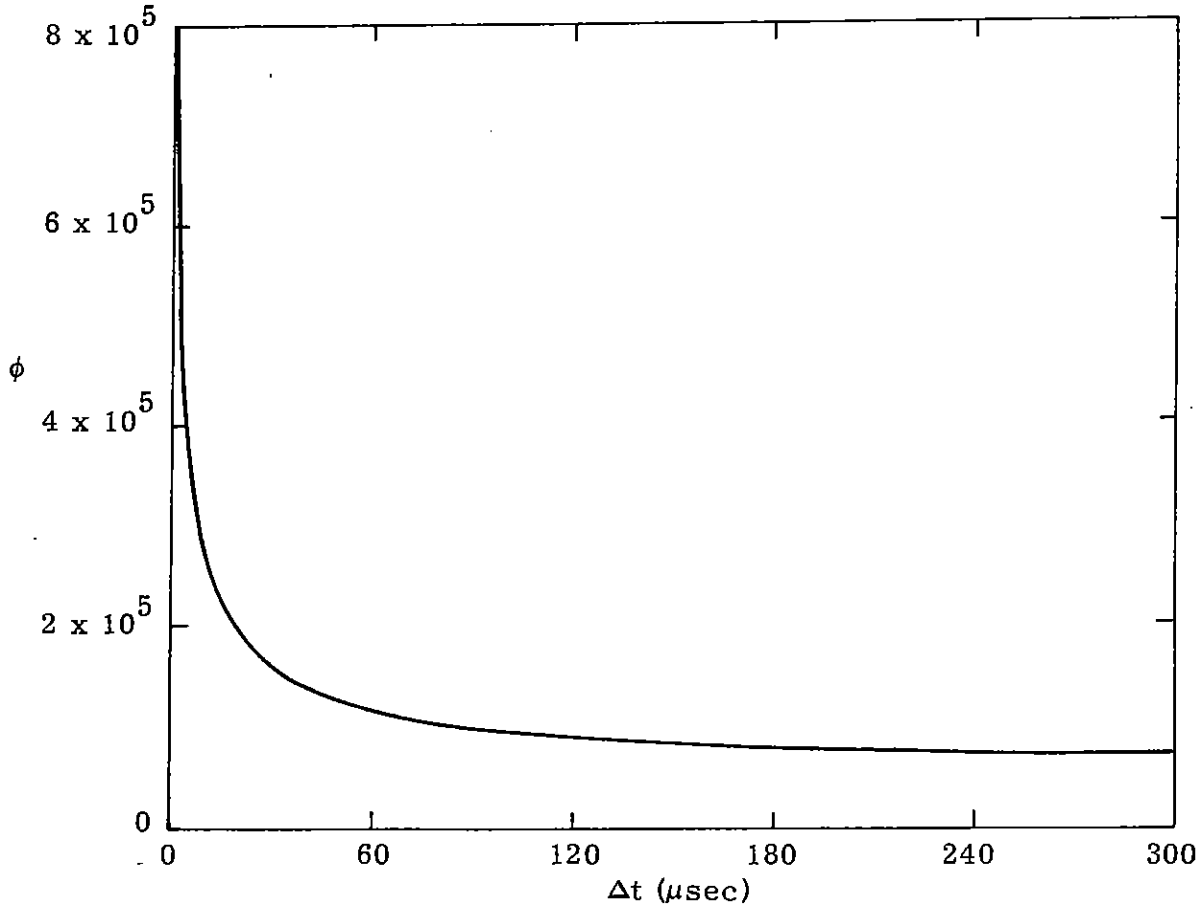

Figure 4.8. Dispersed Pulse with Daytime Ionosphere at 300 km

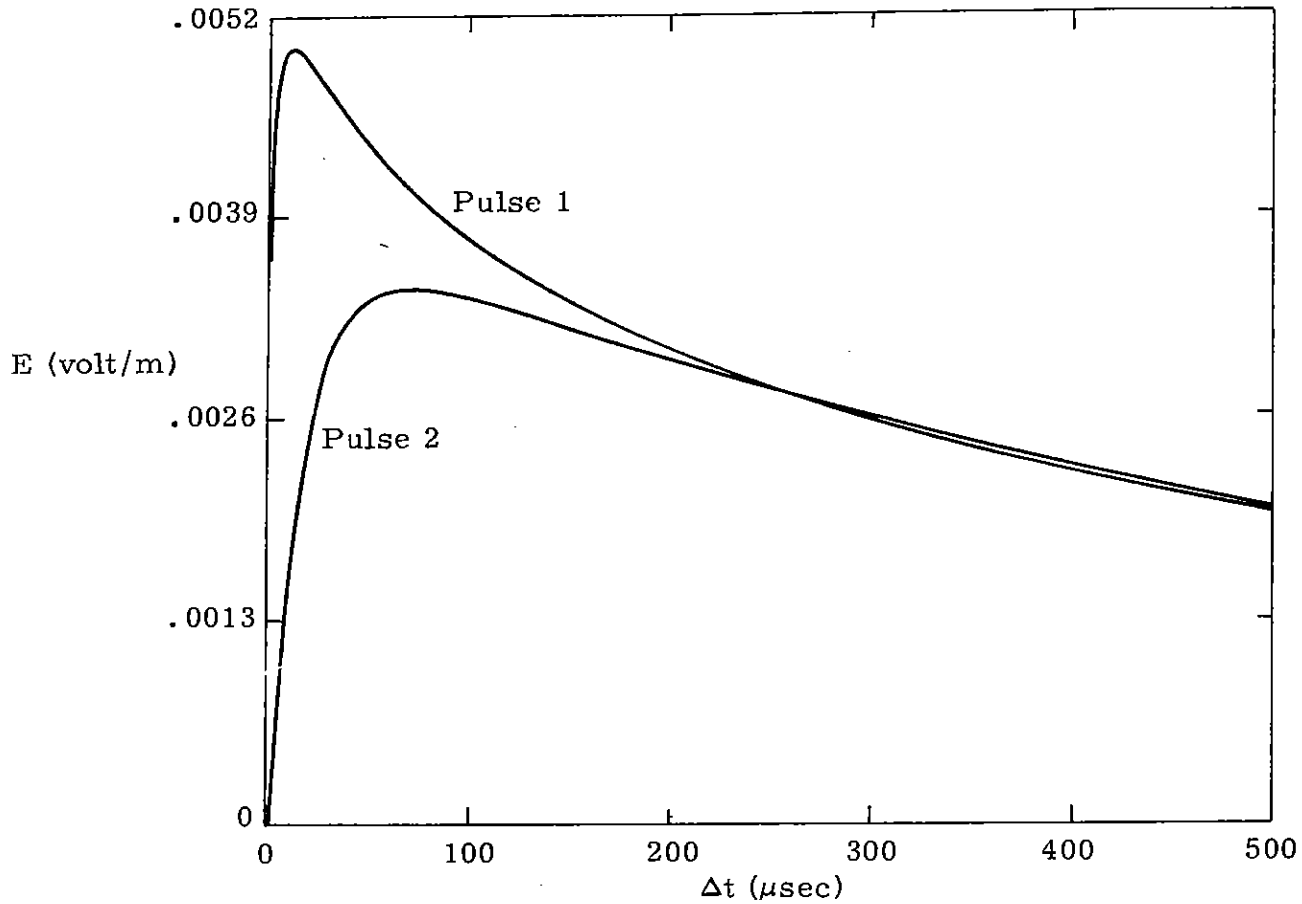

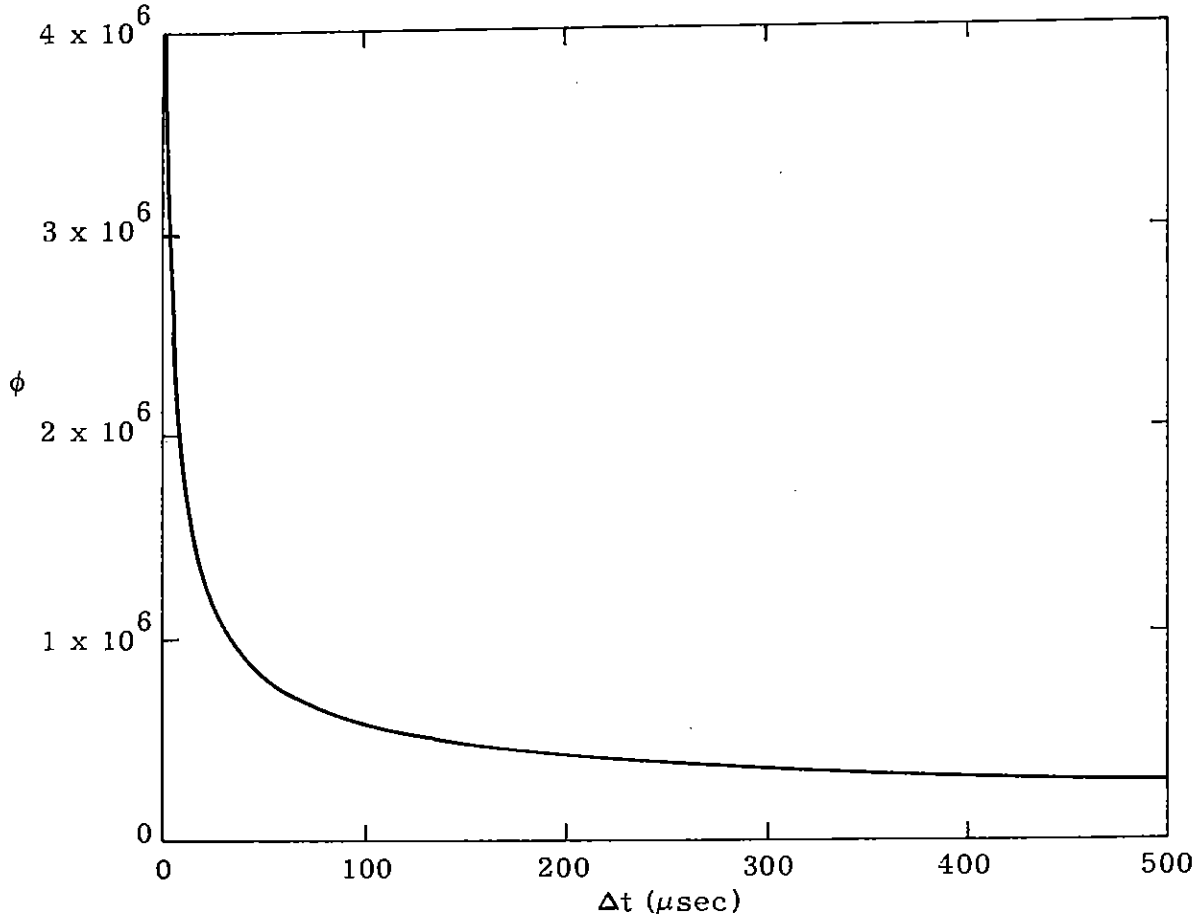

Figure 4.9. Dispersed Pulse with Daytime Ionosphere at 1000 km

5. The Sommerfeld Precursor

The first signal arrives when t is slightly greater than x/c. However, the analysis given in the previous sections is not valid for such an interval of time. Historically, the wavefront of a pulse propagation in dispersive media was first analyzed by Sommerfeld[13] before Brillouin applied the steepest descent method as has been done up to now. The signal near the wavefront is called the "Sommerfeld Precursor."

Let us focus our attention to study the wavefront of (2.4). To achieve this, let us expand n to give

$$\int_o^x n(x', \omega)dx' = \int_o^x [1 - \omega_p^2(x')\omega^2]^{1/2} dx'$$

$$= \int_o^x \left[1 - \frac{\omega_p^2(x')}{2\omega^2} + \frac{3}{8}\frac{\omega_p^4(x')\,c}{\omega^4} + \cdots\right] dx'$$

$$= x - \frac{1}{2\omega^2}\int_o^x \omega_p^2(x')dx' + \frac{3}{8\omega^4}\int_o^x \omega_p^4(x')dx' + \cdots \tag{5.1}$$

On using (5.1) in (2.4), we obtain

$$E(t) = \frac{1}{2\pi}\int_{-\infty}^{\infty}\tilde{g}(\omega)\, e^{i\omega[t-\frac{1}{c}\int_o^x n(x',\,\omega)dx']}\, d\omega$$

$$= \frac{1}{2\pi}\int_{-\infty}^{\infty}\tilde{g}(\omega)\, e^{i[\omega(t-\frac{x}{c})+\frac{1}{2}\int_o^x \omega_p^2 dx'/\omega c-\frac{3}{8}\int_o^x \omega_p^4 dx'/\omega^3 c+\cdots]}\, d\omega \tag{5.2}$$

Let

$$\int_o^x \omega_p^2 dx' = N_2 \tag{5.3}$$

$$\int_o^x \omega_p^4 dx' = N_4 \tag{5.4}$$

(5.2) reduces

$$E(t) = \frac{1}{2\pi}\int_{-\infty}^{\infty}\tilde{g}(\omega)\, e^{i\left[\omega(t-\frac{x}{c})+\frac{N_2}{2\omega c}-\frac{3N_4}{8\omega^3 c}\right]}\, d\omega \tag{5.5}$$

For pulse 1 with $\tilde{g}(\omega)$ given by (4.2) we can expand the last term in the exponent of (5.5) to give

$$E(t) = E^o + \delta E^1 + \frac{\delta^2}{2}E^2 + \cdots \tag{5.6}$$

Here

$$\delta = \frac{3N_4}{8c} , \tag{5.7}$$

$$E^o = \frac{E_o}{2\pi} \int_{-\infty}^{\infty} \left(\frac{1}{\beta + i\omega} - \frac{1}{\alpha + i\omega} \right) e^{i\omega\tau + i\frac{N_2}{2c\omega}} d\omega \tag{5.8}$$

$$E^1 = \frac{E_o}{2\pi} \int_{-\infty}^{\infty} \left(\frac{1}{\beta + i\omega} - \frac{1}{\alpha + i\omega} \right) \left(\frac{1}{i\omega} \right)^3 e^{i\omega\tau + i\frac{N_2}{2c\omega}} d\omega \tag{5.9}$$

$$E^2 = \frac{E_o}{2\pi} \int_{-\infty}^{\infty} \left(\frac{1}{\beta + i\omega} - \frac{1}{\alpha + i\omega} \right) \left(\frac{1}{i\omega} \right)^6 e^{i\omega\tau + i\frac{N_2}{2c\omega}} d\omega \tag{5.10}$$

with

$$\tau = t - \frac{x}{c}$$

To integrate (5.8) through (5.10) it is necessary to make use of the identity[3]

$$J_v(z) = -\frac{\left(\frac{1}{2}z\right)^v}{2\pi} \int_{-\infty}^{\infty} (it)^{-v-1} e^{i\left(t + \frac{z^2}{4t}\right)} dt \tag{5.11}$$

Let

$$g_1^o = \frac{E_o}{2\pi}\int_{-\infty}^{\infty} \frac{1}{\beta + i\omega}\, e^{i\omega\tau + i\frac{N_2}{2c\omega}}\, d\omega \qquad (5.12)$$

Similarly, denote the second term in (5.8) by g_2^o.

Then, one can show that

$$e^{-\beta\tau}\frac{d}{d\tau}(g_1^o\, e^{\beta\tau}) = e^{-\alpha\tau}\frac{d}{d\tau}(g_2^o\, e^{\alpha\tau})$$

$$= E_o\left(\frac{N_2}{2\tau c}\right)^{1/2} J_1\left[\left(\frac{2N_2\tau}{c}\right)^{1/2}\right] \qquad (5.13)$$

E^o is then given by

$$E^o = g_1^o - g_2^o \qquad (5.14)$$

Similarly,

$$E^1 = g_1^1 - g_2^1 \qquad (5.15)$$

with

$$e^{-\beta\tau}\frac{d}{d\tau}(g_1^1\, e^{\beta\tau}) = e^{-\alpha\tau}\frac{d}{d\tau}(g_2^1\, e^{\alpha\tau})$$

$$= -E_o\left(\frac{2c\tau}{N_2}\right) J_2\left[\left(\frac{2N_2\tau}{c}\right)^{1/2}\right] \qquad (5.16)$$

$$E^2 = g_1^2 - g_2^2 \tag{5.17}$$

with

$$e^{-\beta\tau}\frac{d}{d\tau}(g_1^2\, e^{\beta\tau}) = e^{-\alpha\tau}\frac{d}{d\tau}(g_2^2\, e^{\alpha\tau})$$

$$= -E_o\left(\frac{2c\tau}{N_2}\right)^{5/2} J_5\left[\left(\frac{2N_2\tau}{c}\right)^{1/2}\right] \tag{5.18}$$

Substitution of (5.14), (5.15), and (5.17) into (5.6) gives the Sommerfeld Precursor for pulse 1.

Figures 5.1 through 5.4 give the Sommerfeld Precursors for pulse 1 at four altitudes for daytime and nighttime ionospheres. Note that the oscillation near the wavefront follows that of $J_1(x)$, with $x = (2N_2\tau/c)^{1/2}$. Thus, the higher the altitude the larger N_2, which results in fast oscillations. This is confirmed by the increase in oscillations from a scale of 10^{-6} sec to 10^{-10} sec from an altitude of 100 Km to 1000 Km.

For pulse 2, we make the following observations. At 100 Km, the contribution to the wavefront for pulse 1 comes essentially from $E_o\, e^{-\beta t}$ of the original signal. One can expand the undispersed pulse 2 to obtain

$$g(t) = E_o d\, e^{\alpha t_o}\, e^{-(\beta-\alpha)(t-t_o)}\left[1 + e^{-\beta(t-t_o)}\right]^{-1}$$

$$= E_o d\, e^{\beta t_o}\, e^{-(\beta-\alpha)t} + \cdots \tag{5.19}$$

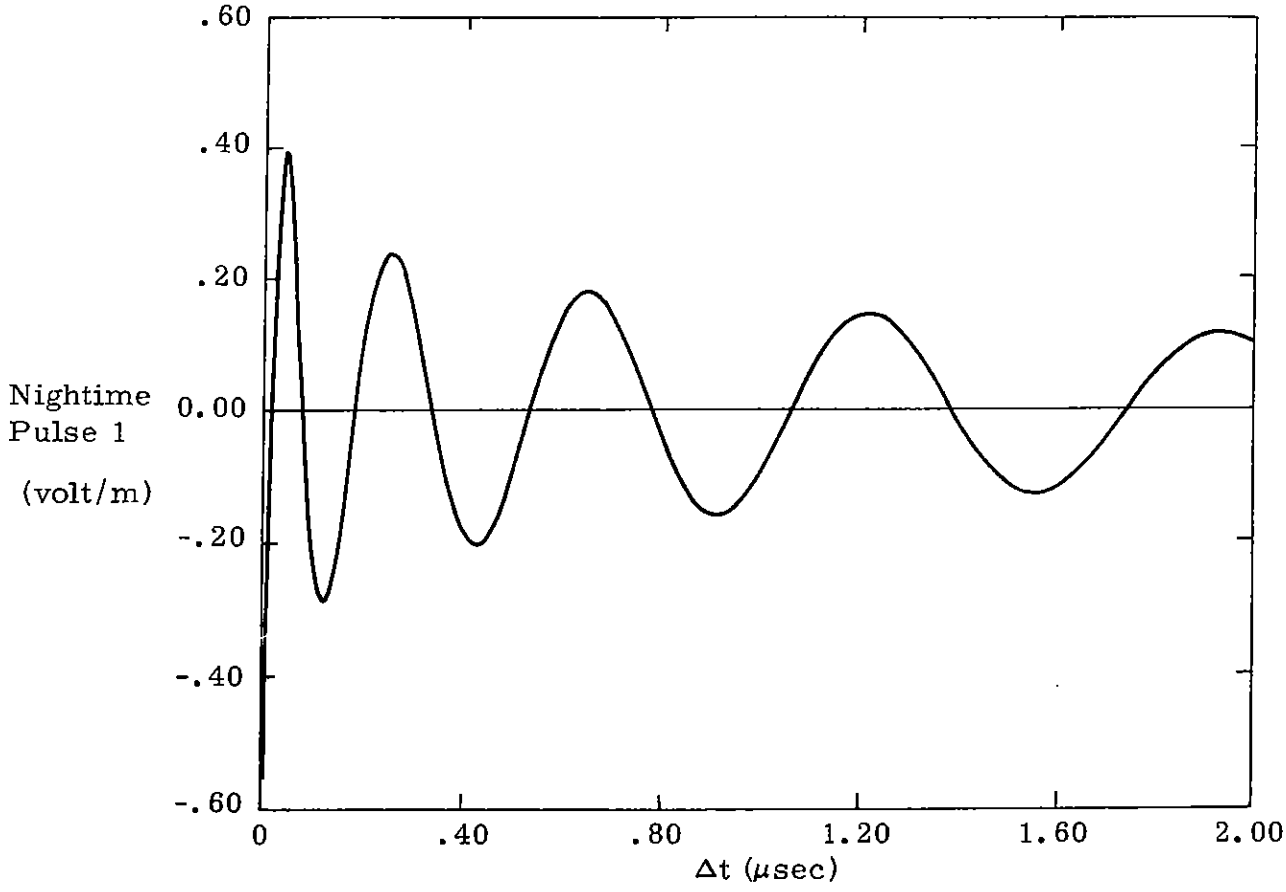

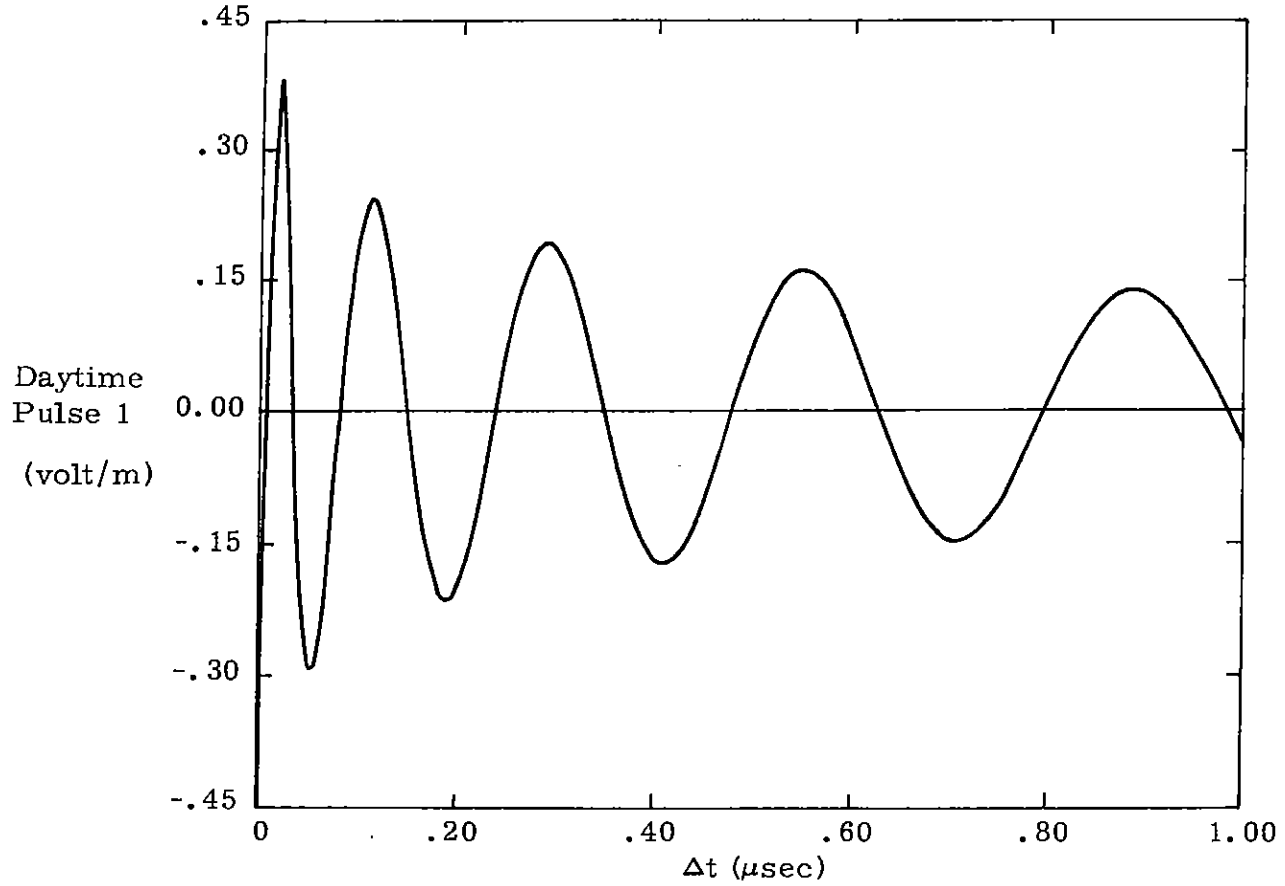

Figure 5.1. Wavefront of Pulse 1 for 100 km

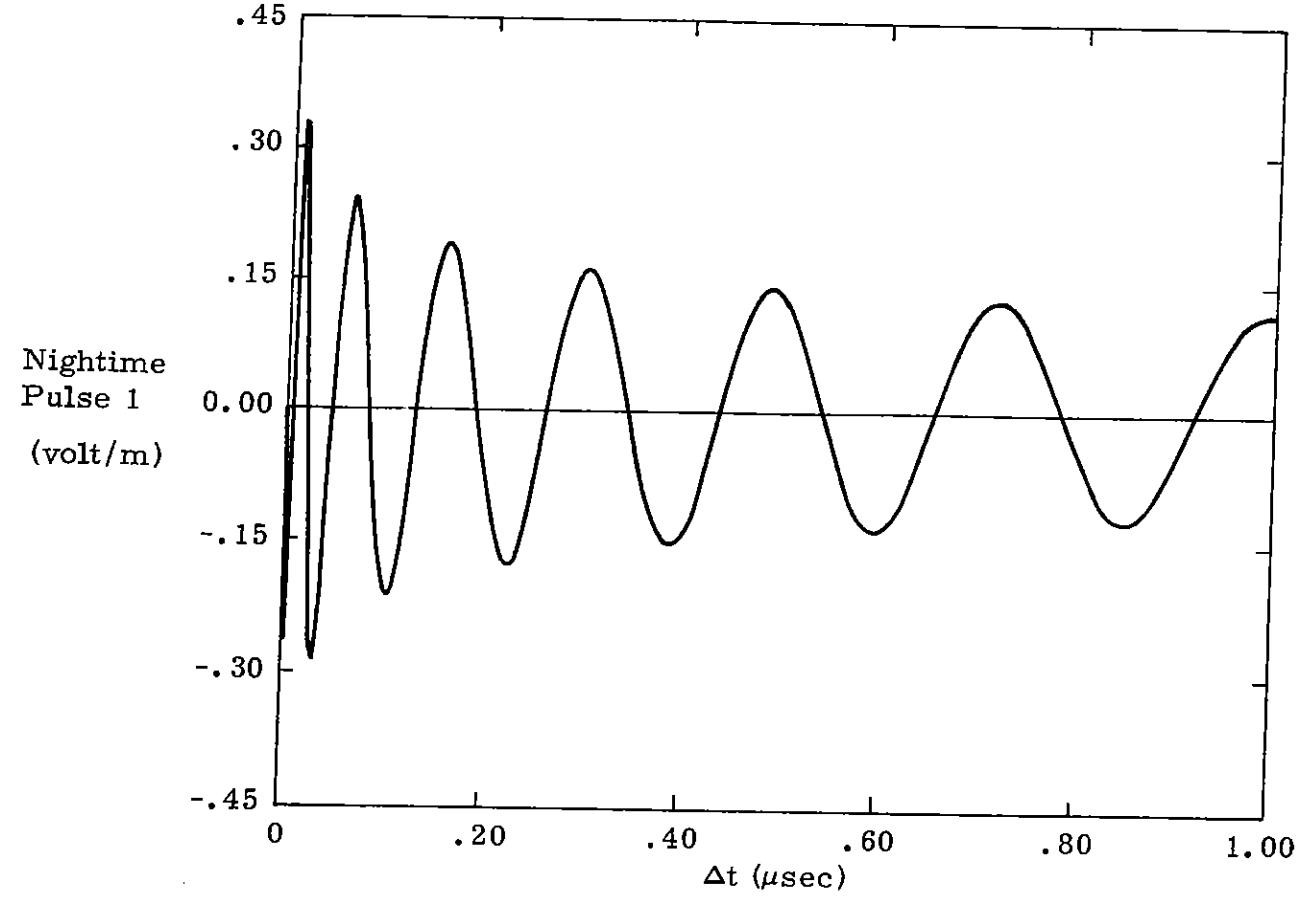

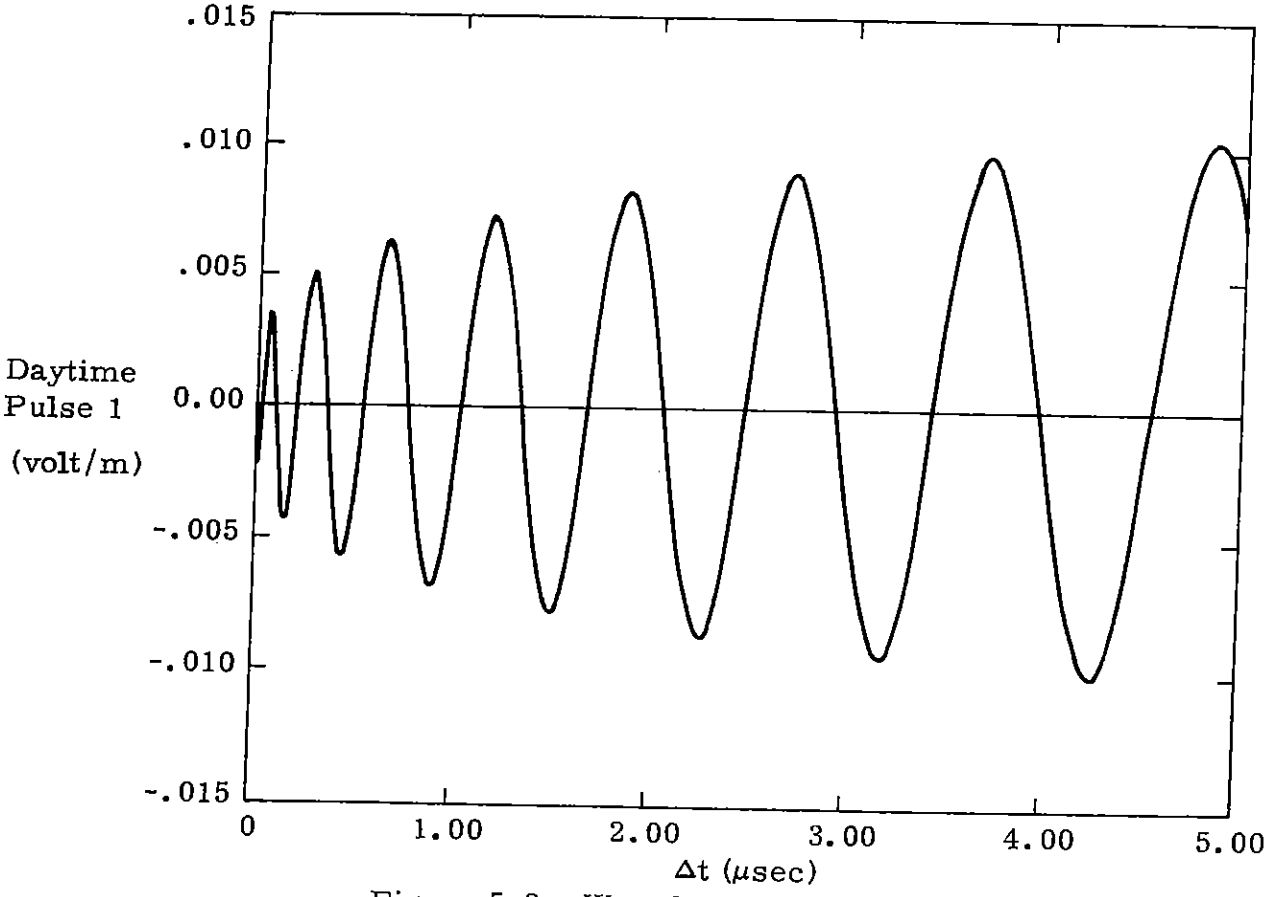

Figure 5.2. Wavefront of Pulse 1 for 200 km

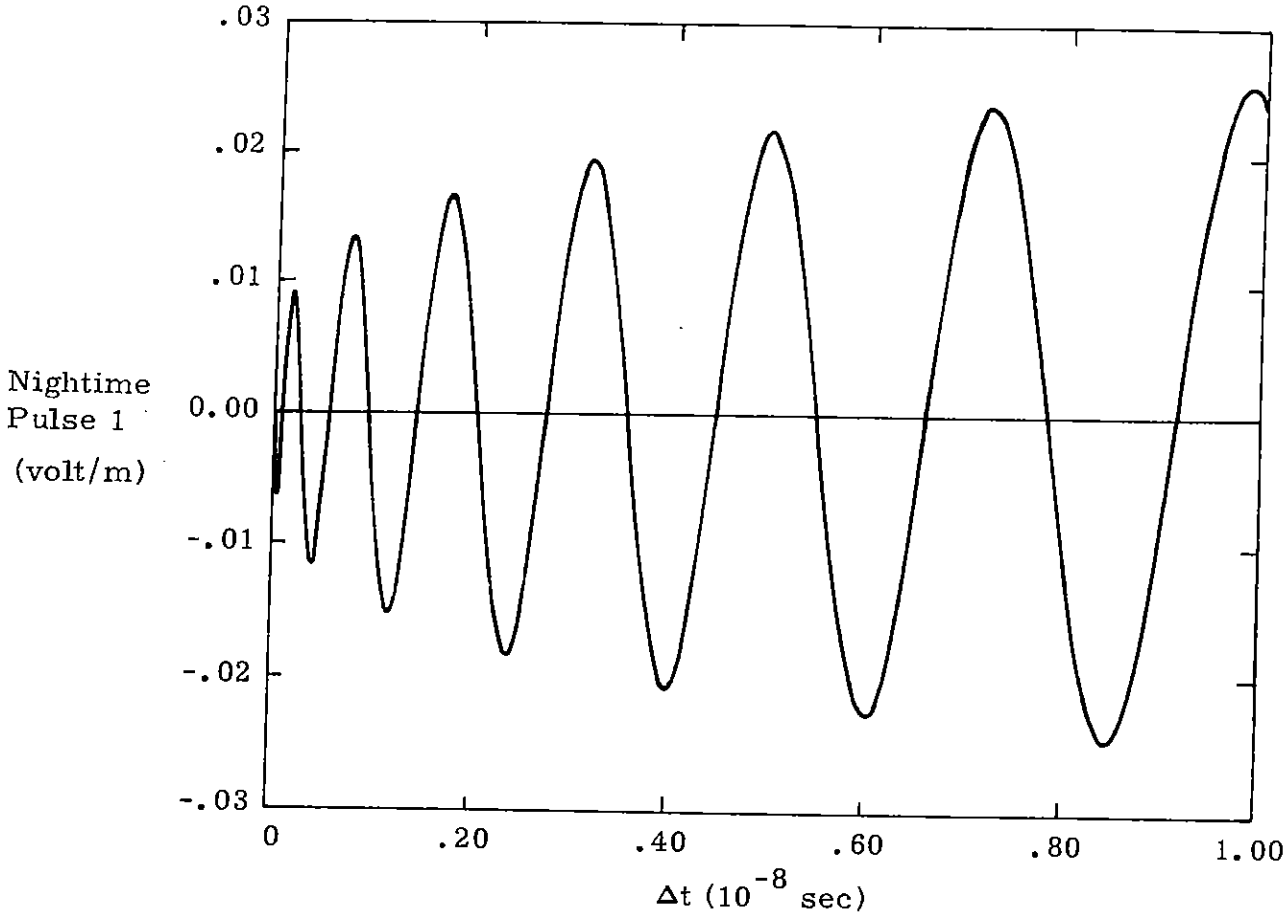

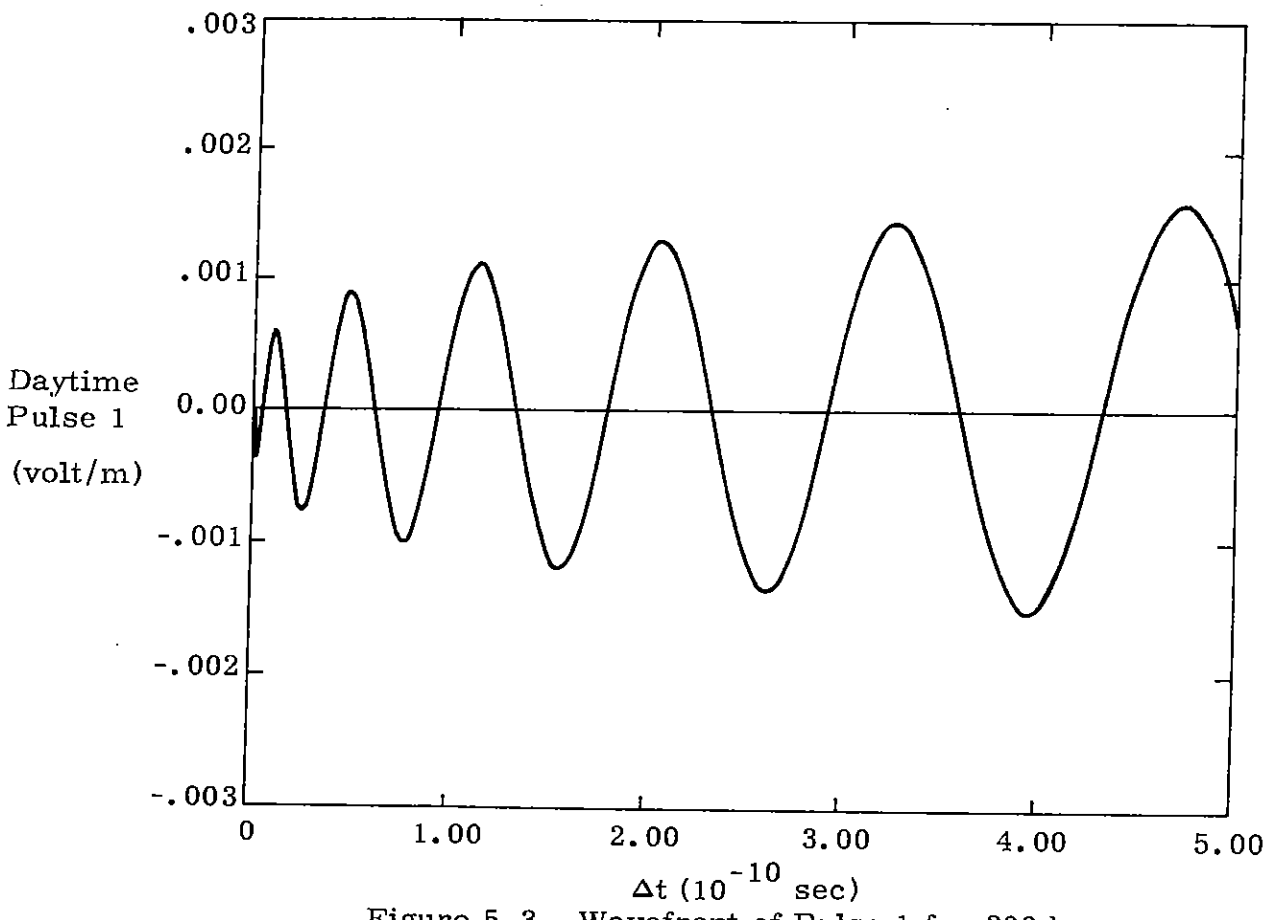

Figure 5.3. Wavefront of Pulse 1 for 300 km

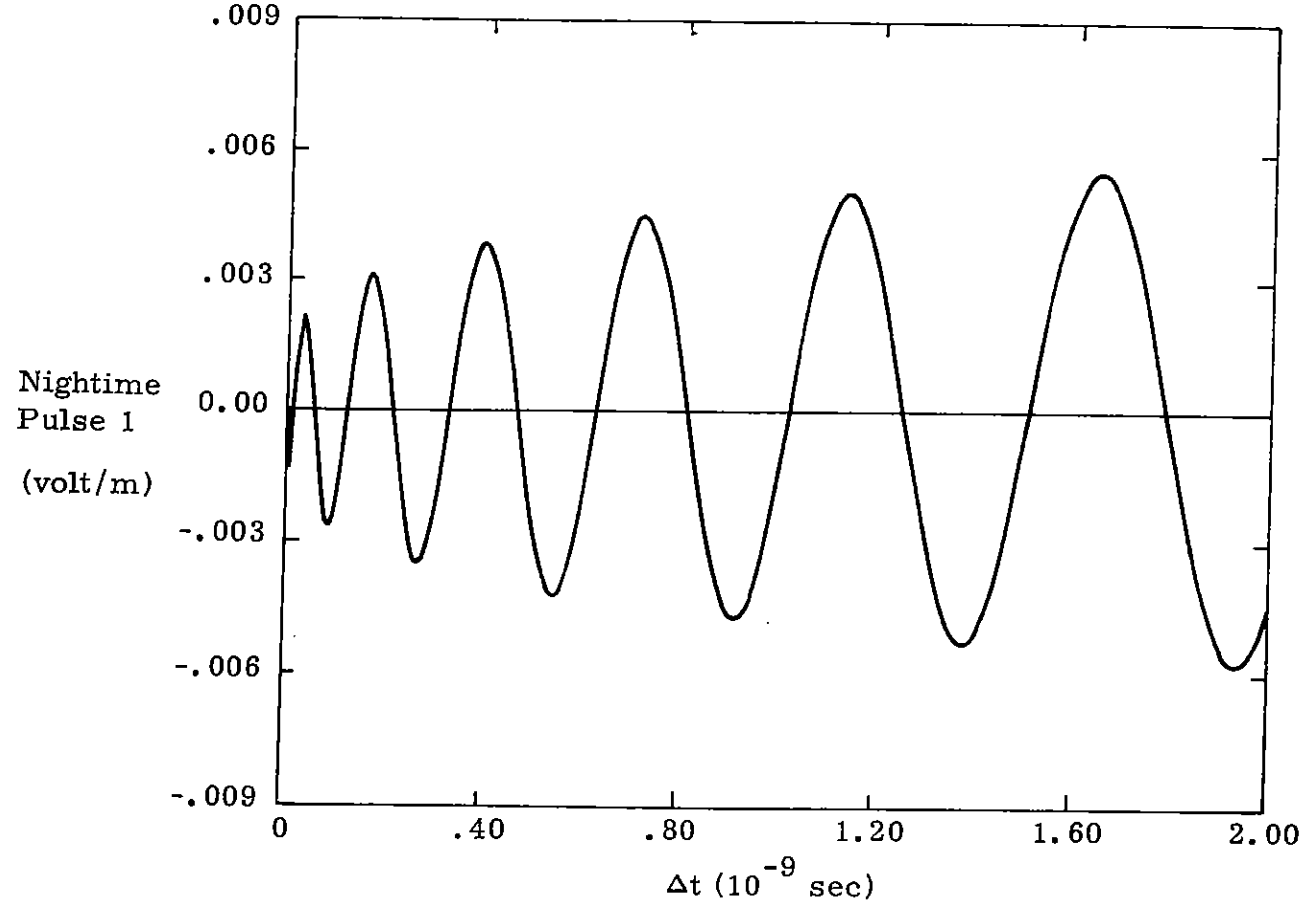

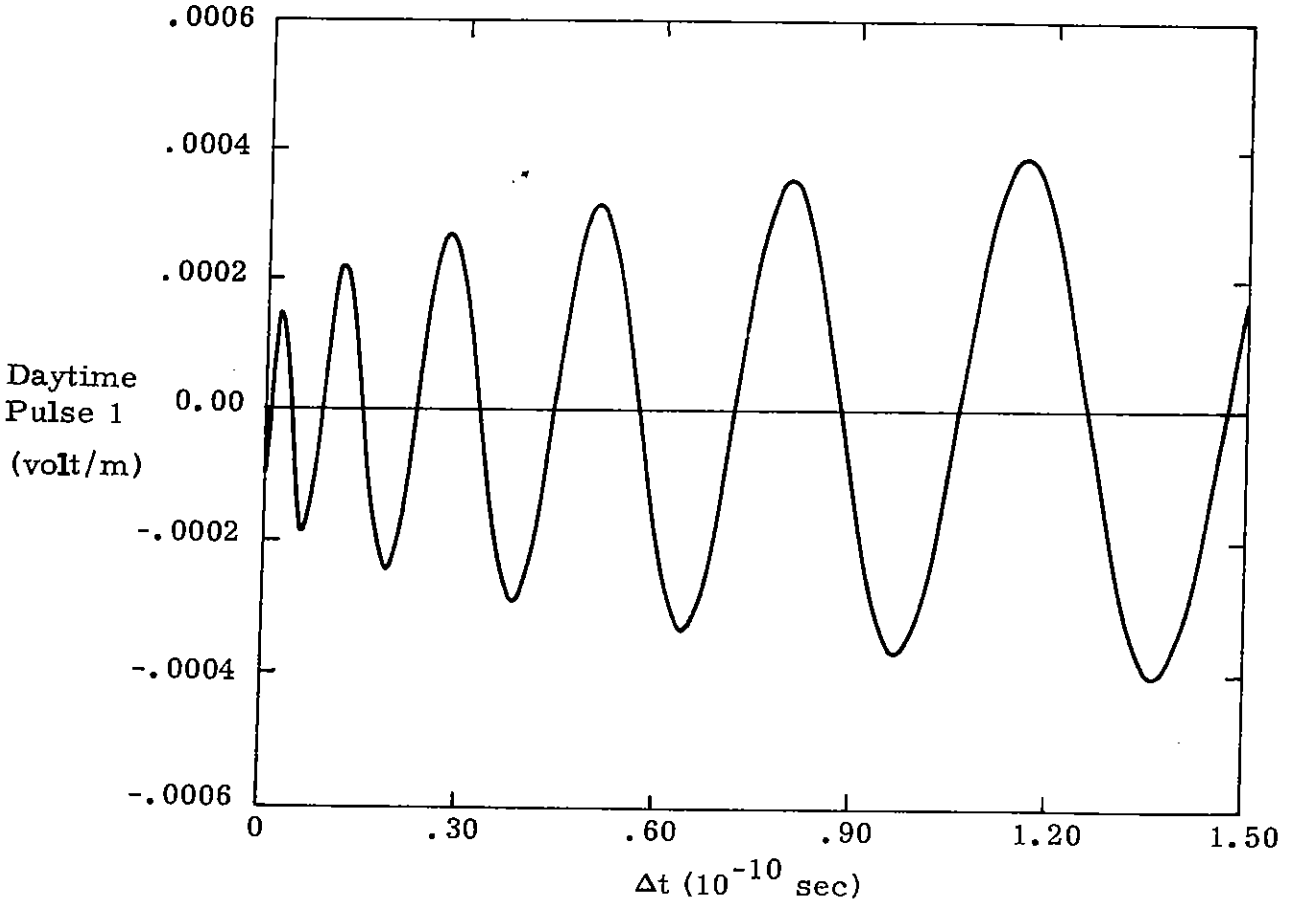

Figure 5.4. Wavefront of Pulse 1 for 1000 km

Again the fast rising input gives a negligible contribution to the Sommerfeld Precursors. Therefore, both pulses have almost identical wavefronts. Note α, β given for pulses 1 and 2 are different.

At 200 Km, 300 Km, and 1000 Km, the magnitudes of the initial wavefront are so small that we do not give them. This can be seen from the spectrum of pulse 2 given in Fig. 4.1. In brief, the initial oscillation of pulse 1 gives us the lower limit of the high frequency contribution to the wavefront. At 200 Km, this lower limit can be estimated from Fig. 5.2 to be 10^9. Referring to the spectrum of pulse 2 given in Fig. 4.1, we see that the spectrum above 10^9 is essentially zero. This leads to the result that the wavefront is small.

6. Concluding Remarks

In this note methods for calculating important features of dispersed EMP in the ionosphere are described. Sommerfeld Precursors are employed to obtain the immediate wavefront of the dispersed signal. Subsequently, the envelope and phase are calculated by the steepest descent integration and these should be valid to great accuracy after a few oscillations of the initial dispersed pulse. The calculations are carried out for nighttime and daytime ionospheres at four different altitudes.

Appendix

In this appendix, the transform of pulse 2 is derived by the residue technique. The time domain waveform of pulse 2 is given by

$$g(t) = \frac{E_o d\, e^{\alpha t}}{1 + e^{\beta(t-t_p)}}, \tag{4.3}$$

By definition, its Fourier transform can be obtained as follows:

$$\tilde{g}(\omega) = \int_{-\infty}^{\infty} g(t)\, e^{i\omega t}\, dt$$

$$= \int_{-\infty}^{\infty} \frac{E_o d\, e^{\alpha(t-t_p)+i\omega(t-t_p)}}{1 + e^{\beta(t-t_p)}}\, dt\, e^{\alpha t_p + i\omega t_p}$$

$$= -\frac{2\pi i E_o d}{\beta} \sum_n e^{i(\alpha+i\omega)(2n+1)\frac{\pi}{\beta}}\, e^{(\alpha+i\omega)t_p}$$

$$= -\frac{2\pi i E_o d}{\beta} \frac{e^{i(\alpha+i\omega)\frac{\pi}{\beta}}\, e^{(\alpha+i\omega)t_p}}{1 - e^{i(\alpha+i\omega)\frac{2\pi}{\beta}}}$$

$$= \frac{\pi E_o d}{\beta} \frac{e^{(\alpha+i\omega)t_p}}{\sin(\alpha + i\omega)\frac{\pi}{\beta}} \tag{4.4}$$

$$= \frac{\pi E_o d}{\beta} \frac{e^{\alpha t_p} e^{i\phi + i\omega t_p}}{\left[\sin^2 \frac{\pi\alpha}{\beta} \cosh^2 \frac{\pi\omega}{\beta} + \cos^2 \frac{\pi\alpha}{\beta} \sinh^2 \frac{\pi\omega}{\beta}\right]^{1/2}} \qquad (4.5)$$

with

$$\tan\phi = \frac{\tan\frac{\alpha\pi}{\beta}}{\tanh\frac{\omega\pi}{\beta}} \qquad (4.6)$$

In the derivation, the integration has been evaluated by the summation of the residue contributions due to all simple poles, and the subsequent geometric series is summed to give a simple formula, (4.4).

References

1. M. A. Messier, "The Ionospherically Propagated Extraatmospheric EMP Environment," Theoretical Note 163, 25 Jan 1972.

2. J. E. Brau, G. H. Canavan, L. A. Wittwer, and A. E. Greene, "Propagated EMP from Tangent and Buried Bursts," Theoretical Note 197, November 1973.

3. K. G. Budden, Lectures on Magneto-ionic Theory, Gordon and Breach, New York, 1964.

4. L. B. Felsen, "Transient in Dispersive Media, I, Theory," IEEE Trans. Ant. Prop., AP-17(2), 191.

5. K. C. Chen and J. L. Yen, "On Steepest Descent Evaluation of an Integral Describing Transient Wave Propagation in Anisotropic Plasmas," Radio Science, Vol. 7, No. 6, 681, June 1972.

6. G. E. K. Lockwood, "Plasma and Cyclotron Spikes Phenomena Observed in Top-Side Ionograms," Can. J. Phys., 41, 190, 1963.

7. M. H. Inston and A. R. Curtis, "Digital and Analogue Computations of Electromagnetic Ray Paths in the Ionosphere Using Euler's Equations for Fermat's Principle," Theoretical Note 143.

8. M. H. Inston and A. R. Curtis, "The Effect of Sporadic E on Ionospheric Pulse Dispersion," Theoretical Note 147.

9. A. R. Curtis, "Digital Computation of the Dispersion of H.F. Pulses Caused by Ionospheric Reflection," Theoretical Note 148.

10. M. H. Inston, "On the Structure and Analysis of a Waveform Produced by Multiple Reception of EM Impulse Dispersed by Ionospheric Reflection," Theoretical Note 151.

11. R. D. Jones, "On Quasi-Monochromatic Signals Propagated Through Dispersed Channels," Theoretical Note 127.

12. G. F. Carrier, M. Krook, and C. E. Pearson, Functions of a Complex Variable, New York: McGraw-Hill, 1966.

13. L. B. Brillouin, Wave Propagation and Group Velocity, New York: Academic Press, 1960.